

POLITECNICO DI TORINO

Corso di Laurea Magistrale
in Ingegneria Aerospaziale



Sensitive Analysis of Mistuned Bladed disk

- Tesi di Laurea Magistrale -

Student:

Orlando Giulio

Supervisors:

Prof. Daniele Botto

Prof. Urlapkin, Aleksandr V.

2018/2019

”That’s one small stem for a man,
one giant reap for his humanity”

Contents

Abstract	2
1 Chapter 1	
Dynamic Analysis of Bladed disk of Compressor	3
1.1 Entire Structure	8
1.2 Single Sector	13
2 Chapter 2	
Forced Response Analysis	18
2.1 Entire Structure	21
2.2 Single Sector	27
3 Chapter 3	
Mistuning Analysis	28
3.1 What is the Mistuning?	28
3.2 Simplified model	30
4 Chapter 4	
Simplified Calculation of Eigenvalues Derivatives	45
4.1 Non-repeated roots	45
4.2 Repeated roots	48
5 Conclusion	50
Appendices	51
A Matlab script	51
References	56

List of Figures

1	Rotor Wheel Examples	3
2	Cyclic Symmetry Examples	4
3	Examples of Orthogonal mode shape for a couple of frequencies on a membrane for 1x0 Mode Shape and 3x0 Mode Shape	5
4	Example Sinusoidal trend of eigenvectors for one nodal diameter	6
5	Example of opposite sinusoidal for $f_1 = 97.9933$ Hz on the left and $f_2 = 306.4267$ Hz on the right.	6
6	Sector of a disk	7
7	Model of Entire Structure	8
8	Umbrella mode for $\{\psi_0\}$ on the left and $\{\psi_{N/2}\}$ on the right	11
9	Umbrella mode in 3D [6]	11
10	"Disk Dofs" on the left and "Blades Dofs" on the right	12
11	"Disk Dofs" on the left and "Blades Dofs" on the right	12
12	Model of single sector	13
13	Mode Shape 4x0 without nodal circles	16
14	Mode Shape 4x1 with nodal circles	16
15	Frequency and Engine Order comparison	19
16	Excitation Force	20
17	Example of Force Response with EO=2 for disk	22
18	Example of Force Response for EO=1 for disk with different Modal Damping Ratio/	23
19	Example of Force Response for EO=1 for Disk.	24
20	Example of Force Response for EO=1 for Blade.	24
21	Zoom of Resonance in the Disk at EO=1.	25
22	Diminution of Resonance in the Disk at different EO.	25
23	Force Response at different EO.	26
24	Comparison of Full-System and Cyclic Symmetry Response for EO=2	27
25	The Simplified Model for the analysis	30
26	Mesh of the Simplified Model	31
27	Definition of Lumped Component	32
28	two sectors	34
29	three sectors	36
30	Twenty-three Sectors	38
31	Twenty-four Sectors	40

32	Global Stiffness Matrix K	41
33	Global Mass Matrix M	41
34	Results of Nelson's Method	47
35	Results of Ojalvo's Method	48

Abstract

The aeronautics sector in that it is facing increasingly difficult challenges for which the keyword at the base of each principle is "Security". Security does not mean an absence of errors but the maximum limitation of them. This is because the percentage of error cannot be eliminated, and this statement is further legitimized if also human factor acts in transactions. The process of implementing a damage identification strategy for aerospace engineering infrastructure is referred to as structural health monitoring (SHM). The damage can be defined as changes introduced into a system that adversely affect its current or future performance. The term damage does not necessarily suggest a total loss of system functionality, but rather that the system is no longer operating in its optimal manner. So, as the damage grows, it will reach a point where it influences system operation to a point that is no longer acceptable to the user. This point is referred to as a failure. The Engine, compressor, in this case, is one of the most stressed parts of an Aircraft because high rotational speed creates a field of vibration that it needs to be controlled and checked. This project of the thesis will develop an analysis of a dynamic structure of a section of a Rotor wheel of a compressor. This analysis will be treated through the chapters in order to show all the main faceting of the theme. The section of the compressor is an axisymmetric structure and this helps computer programs on the analysis. But The Rotor part of turbomachinery is a very complex structure. The FEM analysis required a high computational cost of calculation so is needed a model simplification without any loss of accuracy. It is possible to reach this target using the cyclic symmetry of a rotationally periodic structure that lets to analyze only one sector generalizing the results to all the structure. These types of elements are always characterized by the presence of double natural frequencies, corresponding to the twin mode shape counter-rotating along with the system. These characteristics will be discussed. Compressor rotors are dynamical systems designed to have identical blades but, in reality, there are random deviations among the blades caused by material defectiveness, manufacturing tolerances, wear and other causes. This destroys the cyclic symmetric conditions of the structure and is called Mistuning. The rotation of the bladed disk in turbomachines are exposed to large static and dynamic stresses. Static loads mainly arise from centrifugal forces and thermal strains while forced vibrations are caused by actuating air pressures and rotor imbalances. Mistuning caused an unexpected increase in maximum stresses that can lead to premature high cycle fatigue of the blades and failure problems. The main purpose of the thesis will be to find a way how to predict and evaluate these effects. Chapter 1 shows an introduction of the symmetric full structure of which a dynamic analysis will be performed with two methods: full structure and one sector following the theory of Thomas. To do it a simplified lumped model

will be created. A study of nodal diameter will be performed investigating the main difference between the two methods. In Chapter 2 the study will continue by applying an external force in the structure and monitoring the force response on it. This will be done in both ways to better understand the behavior of the structure and how the vibration process will change. In Chapter 3 the Mistuning Condition will be applied. But first of all, a simplified 3D model will be created on Ansys in order to obtain Stiffness and Mass matrices of the structure. The results than could be expanded to a complex model. After this, the percentage error between the normal case and the mistuned one will be analyzed. Chapter 4 will be introduced two new simpler methods to predict the mistuning effect in an easy way. Then a comparison between the two methods will be done.

1 Chapter 1

Dynamic Analysis of Bladed disk of Compressor

The subject of the thesis will be a bladed disk or general rotor wheel of a compressor. The main goal will be to analyze the behavior of physical structure when subjected to force that generates a vibration in all the structure. The Force could be a load of different nature that acts on the structure with different accelerations. This acceleration is compared to the *natural frequency* of the structure. First of all, it's important to define what is a natural frequency. Briefly, the bladed disk structure vibrates in a natural way without any damping forced. The frequency at which vibrates is the natural frequency. The analysis will be a static one if the load's acceleration is sufficiently slowly in comparison with the natural frequency. In the opposite case, such as in the presence of dynamics loads, it should be applied a dynamic analysis of the structure. This second approach will be used. This type of analysis is used to find out the dynamic displacements, the time history and the modal analysis. The modal analysis lets to study the dynamic characteristics in the frequency domain. This process identifies modal properties. To better understand the bladed disk behaviour a very important step is to specify these modal properties such as natural frequencies and modal shapes. A modal shape is a standing wave state of excitation, in which all the components of the system will be affected sinusoidally under a specified fixed frequency. Of course, in reality is not possible to have a system that perfectly fits under a standing wave framework, so the modal shape is a concept used for a general characterization of specific states of oscillation. In general to indicate a Mode Shape it is used the notation $D \times C$ where D is the number of Nodal Diameter and C the number of Nodal Circle. An example is showed in the next paragraph.



Figure 1: Rotor Wheel Examples

Any point of the structure that doesn't move from its position during vibration, it means where the displacement is zero at all times, is called *node*. The mode shape in these points is zero. When the subject treated is a two dimensional system, the nodes became a straight line called *nodal diameter* or a circle line called *nodal circle*. In base of the value of frequency, it is possible to have different mode shapes related to the different number of diameters or circles. To a more valuable understanding of this dynamics characteristics of the structure, it is possible to consider the rotor wheel as a *circular membrane* although it doesn't represent a three-dimensional body. Solving the dynamic problem of the structure allows to calculate *eigenvalues* and *eigenvectors* of the system. To be clear, the eigenvalues are the natural frequencies of vibration, and the eigenvectors are the shapes of these vibrational modes.

Going forward, a structure has a *cyclic symmetry* when the geometry, parameters, constraints and results of a partial model can be copied around an axis in order to give the complete model. The rotor wheel has a cyclic symmetry in the theory. So is possible to isolate and study just one sector, and then expand the results for all the structure. This will be done later.

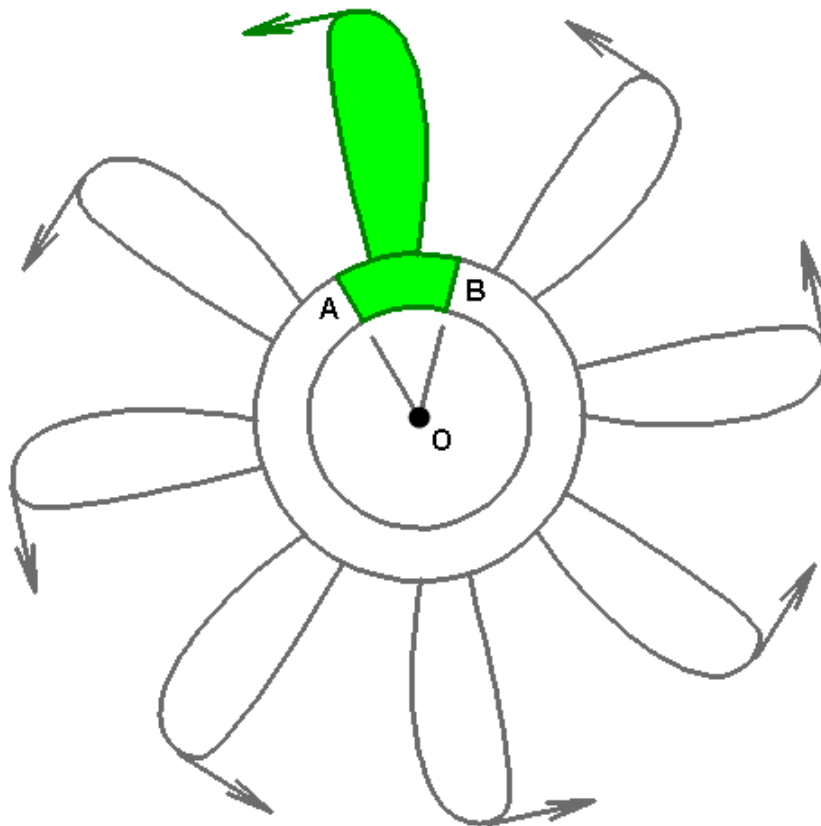


Figure 2: Cyclic Symmetry Examples

The symmetric property gives symmetric matrices that create the system's equation showed later in the chapter. As a solution of a system with symmetric matrices, it should exist a couple of eigenvalues at which the structure assumes the same mode shape but rotated of an angle to form its complementary. This due to the "mutually orthogonal properties of eigenvectors". In the following image are showed two examples of the mode shape with one nodal diameter that occur for low frequencies of vibration.

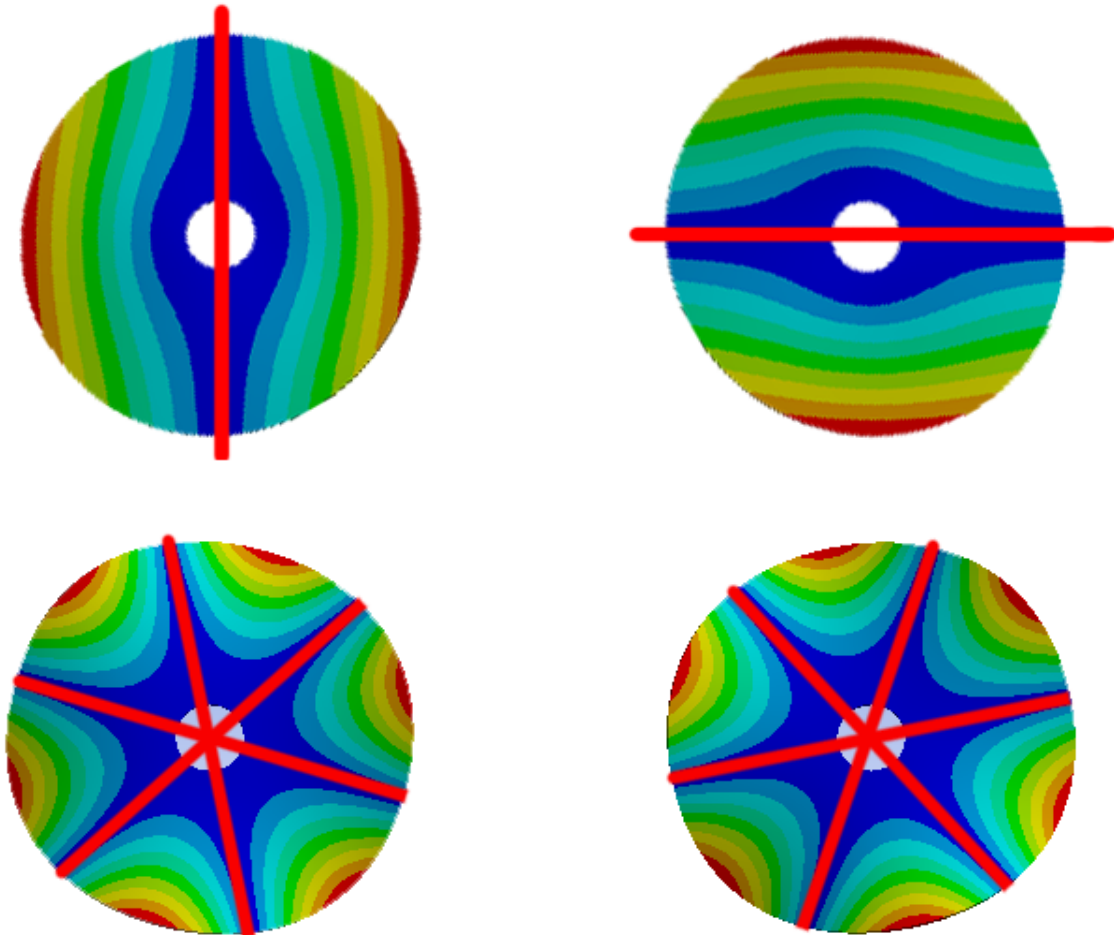


Figure 3: Examples of Orthogonal mode shape for a couple of frequencies on a membrane for 1x0 Mode Shape and 3x0 Mode Shape

It's more simple to understand the *node's* concept looking to the following figure. It represents the sinusoidal shape of eigenvectors that appears plotting the amplitude of these ones over the Number of Sectors of the structure. From the figure is clear that the red points are opposite and related to the second eigenvector and the yellow ones to the third. At these points, the structure never changes its position from the zero amplitude. This example shows the case of Mode Shape 1x0 so with one nodal diameter.

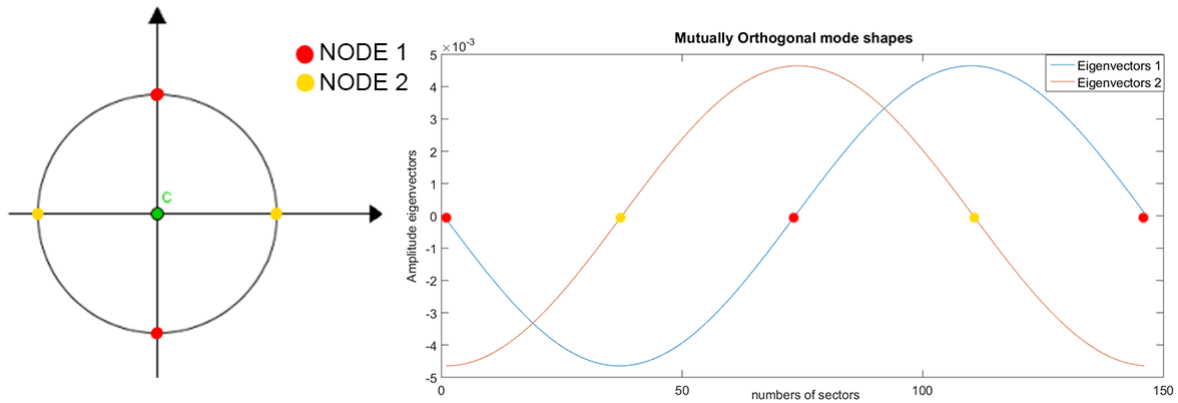


Figure 4: Example Sinusoidal trend of eigenvectors for one nodal diameter

It's important to denote that for low frequency is achievable to study only the presence of nodal diameter. It's possible to see this from the direction of the two sinusoids of a couple of eigenvectors that in this case are in concordance. On the other hand, to a more higher frequency, it is revealed the presence of a nodal circle too. To discover this, the two sinusoids are in opposite direction. This fact is shown in the following figures.

The following example is about the Mode Shape 1x0 for a frequency $f_1 = 97.9933$ Hz and about the Mode Shape 1x1 for a frequency $f_2 = 306.4267$ Hz.

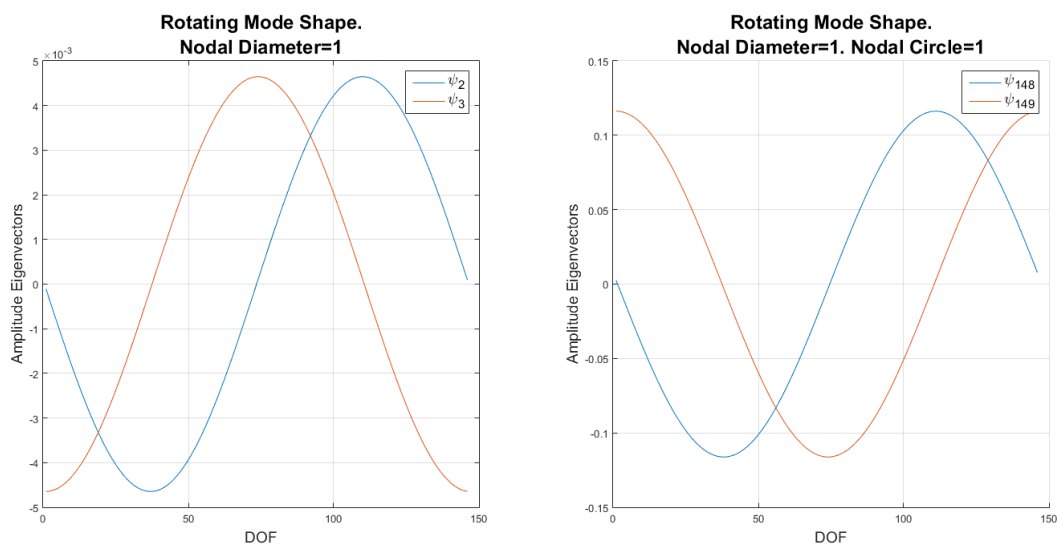


Figure 5: Example of opposite sinusoidal for $f_1 = 97.9933$ Hz on the left and $f_2 = 306.4267$ Hz on the right.

To evaluate the consistency of the nodal circle must do another analysis in a radial direction but this matter is not treated on this paper.

As said, the structure could be divided into a number N of equal sectors in respect of cyclic symmetry. It's possible to find a relation between the number of sectors N and the number of nodal Diameters. First of all, the choice of the sector will coincide with the position of one blade plus the corresponding part of the disk below it. This allows matching the number of sectors with the number of blades. It will be shown that the relation with nodal diameters is associated with the nature of the integer number N , it means if it is even or odd.

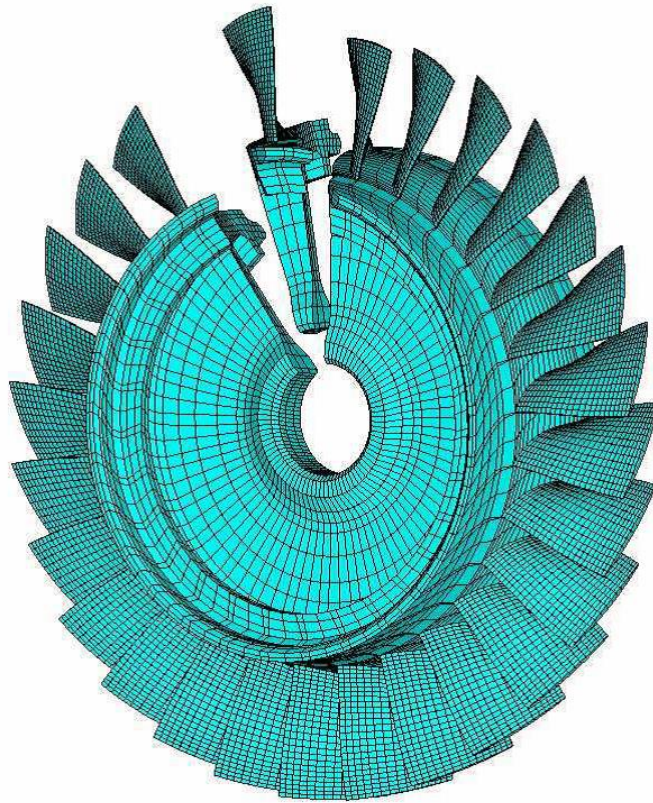


Figure 6: Sector of a disk

The relation between sectors and nodal diameter can be explained through the expression below:

- $0 \leq N \leq \frac{N}{2}$ if N is even;

- $0 \leq N \leq \frac{N-1}{2}$ if N is odd.

After this general introduction of basic concepts of the dynamic system, the next step will be to study a dynamic behavior on the model of the structure that summarises the Bladed disk configuration. A Modal analysis will be done comparing the different response of disk and blades. As the first approach, no external force will be treated but only the difference between a study of the Entire structure and a study of only one sector to expand, at a later time, the analysis to all the structure.

1.1 Entire Structure

The Entire Structure of the Rotor Wheel model was represented as a group of masses concentrated in two points as is possible to observe in Fig. 1. This allows considering the system as lumped. This condition grants to ignore the deformation of each element and, furthermore, creates a diagonal mass matrix and negates the need to integrate mass across the deformed element. It approximates the behavior of the distributed system under certain assumptions. In one point is concentrated the mass of the disk m_d and, on the other point, the mass of the blade m_b . In this case, must be taken into account their mutual connections and their connections to the structure due to different stresses environment. These connections are considered through three stiffness elements such as k_b that link the mass of blade and the mass of disk, k_c that link one mass of disk with the following one and k_d that link the mass of disk to the shaft(the ground). In general, the stiffness is the resistance offered by an elastic body to deformation. This deformation occurs mainly in the disk part so the results is that k_b should be lower than k_c and k_d . These last two stiffnesses were considered equal for a simplification in the system. In this specific case, it was chosen a value of stiffness from an initial value of frequencies. So both for masses and stiffness, the values for disks are three times the values of the disk.

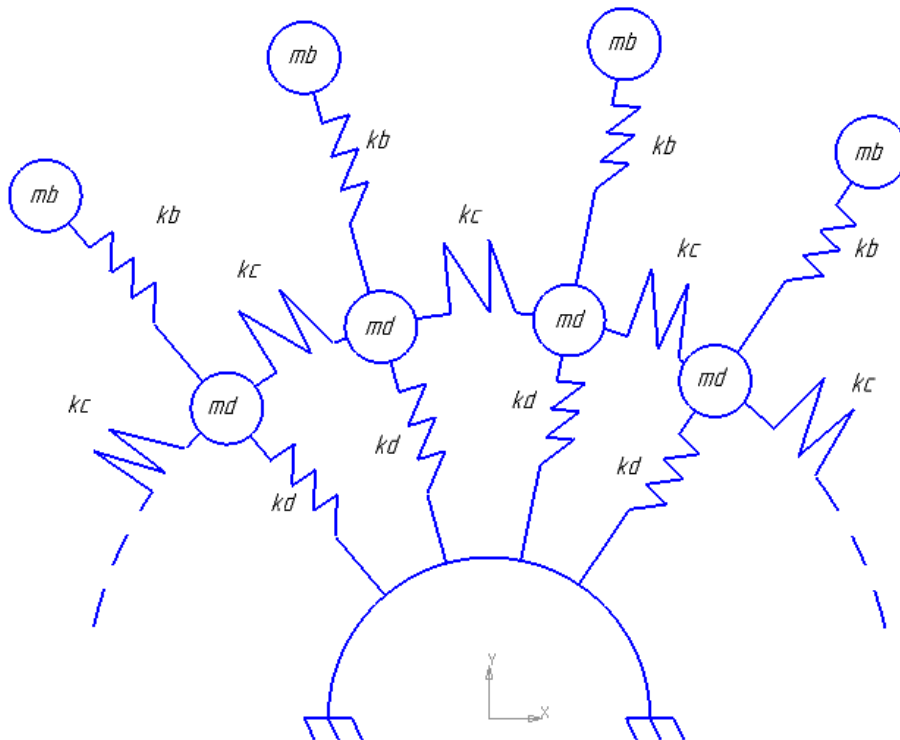


Figure 7: Model of Entire Structure

The way to represent the Entire Structure can be different. The one in Fig. 7 is just a simplified case that it was used to better proceed in the resolution of the dynamic process. The Degrees of Freedom (Dof) of this model are two for each sector, so in total $2N$ if the number of the sector is N . The Dofs are linked to the two masses described before. It means that for the two elements there are a set of parameters that may vary independently.[3]

After this initial description, is possible to determine the system equation that will bring to the modal analysis. In this chapter, the case considered is without the action of external forces so the Force Response will be equal to zero. Even the damping is generally ignored. The general form of eigensystem is:

$$[M]\{\ddot{x}\} + [K]\{x\} = [0] \quad (1.1)$$

where $\{x\}$ represents the displacement of the masses and $\{\ddot{x}\}$ is its acceleration. $[M]$ and $[K]$ are, respectively, $2N \times 2N$ mass matrix and stiffness matrix of the structure. As a general rule, the construction of the master mass matrix $[M]$ largely parallels of the master stiffness matrix $[K]$. Mass matrices for individual elements are formed in local coordinates, transformed to global, and merged into the master mass matrix following exactly the same techniques used for $[K]$. To help for the comprehension of the process of merging, the matrices of individual elements are showed below [2]:

$$M_b = \begin{bmatrix} m_b & 0 \\ 0 & m_b \end{bmatrix} \quad M_d = \begin{bmatrix} m_d & 0 \\ 0 & m_d \end{bmatrix}$$

$$K_b = \begin{bmatrix} k_b & -k_b \\ -k_b & k_b \end{bmatrix} \quad K_c = \begin{bmatrix} k_c & -k_c \\ -k_c & k_c \end{bmatrix} \quad K_d = \begin{bmatrix} k_d & -k_d \\ -k_d & k_d \end{bmatrix}$$

After identifying the matrices of single elements, another important step is the enumeration of the Dofs of the structure. Even the enumeration is arbitrary. In this case, it was considered that the first $\frac{N}{2}$ Dofs are related to the disk and the second one to the blades.

Exists a verification that lets to check if the Matrices are good or not. For the Mass Matrix, it should have: (1) matrix symmetry, (2) physical symmetries (such as element symmetries must be reflected), (3) positivity. For Stiffness Matrix, its properties are: (1) Stiffness matrix is symmetric and square, (2) In stiffness matrix, all diagonal elements are positive, (3) it is positive definite.

The Global Mass and Stiffness Matrices of the Entire Structure are built in this way:

$$[M] = \text{diag}(m_{d_1} \dots m_{d_N}, m_{b_1} \dots m_{b_N}) \quad (1.2)$$

$$[K] = \begin{bmatrix} k_s & -k_c & 0 & \dots & 0 & -k_c & -k_b & 0 & \dots & \dots & \dots & 0 \\ -k_c & \ddots & \ddots & \ddots & 0 & \dots & \dots & 0 & \ddots & 0 & \dots & \dots & 0 \\ 0 & \ddots & \ddots & \ddots & 0 & \dots & \dots & 0 & \ddots & 0 & \dots & \dots & 0 \\ \vdots & 0 & \ddots & \ddots & \ddots & 0 & \dots & \dots & 0 & \ddots & 0 & \dots & 0 \\ 0 & \vdots & 0 & \ddots & \ddots & -k_c & 0 & \dots & \dots & 0 & \ddots & 0 & 0 \\ -k_c & \vdots & \vdots & 0 & -k_c & k_s & 0 & \dots & \dots & \dots & 0 & -k_b & 0 \\ -k_b & 0 & \vdots & \vdots & 0 & 0 & k_b & 0 & \dots & \dots & \dots & 0 & 0 \\ 0 & \ddots & 0 & \vdots & \vdots & \vdots & 0 & \ddots & 0 & \dots & \dots & 0 & 0 \\ \vdots & 0 & \ddots & 0 & \vdots & \vdots & \vdots & 0 & \ddots & 0 & \dots & 0 & 0 \\ \vdots & \vdots & 0 & \ddots & 0 & \vdots & \vdots & \vdots & 0 & \ddots & 0 & 0 & 0 \\ \vdots & \vdots & 0 & \ddots & 0 & \vdots & \vdots & \vdots & 0 & \ddots & 0 & 0 & 0 \\ \vdots & \vdots & \vdots & 0 & \ddots & 0 & \vdots & \vdots & \vdots & 0 & \ddots & 0 & 0 \\ 0 & 0 & 0 & 0 & 0 & -k_b & 0 & 0 & 0 & 0 & 0 & 0 & k_b \end{bmatrix} \quad (1.3)$$

where $k_s = k_d + 2k_c + k_b$

Due to the enumeration $\{x\} = x_i$ where $i \in \{1, N\}$ for disk and $i \in \{N + 1, 2N\}$ for blades.

From Fig. 4 and Fig. 5 it has been anticipated that the solution of the system as the general shape:

$$\{x\} = \{X_0\} \cos(\omega t + \phi) \quad (1.4)$$

with $\{X_0\} \in R^n$ where $\{X_0\}$ is the Amplitude that determines the height of sinusoid (this parameter varies if an external force is applied), ϕ is the phase of the solution and ω is the frequency.

To get the eigenvectors and eigenvalues solution from the system is needed to derivatives two times the general solution:

$$\{\dot{x}\} = \{X_0\} \omega \sin(\omega t + \phi)$$

with $\{X_0\} \in R^n$. This represents the velocity of the system and:

$$\{\ddot{x}\} = -\{X_0\} \omega^2 \cos(\omega t + \phi)$$

with $\{X_0\} \in R^n$. This represents the acceleration of the system. Substituting the acceleration to the system equation is possible to obtain:

$$([K] - \omega^2 [M]) \{X_0\} = 0 \quad (1.5)$$

If the determinant of this equation is set equal to zero, the eigenvalue ω_i^2 is obtained with $i = 1, \dots, 2N$ (note that the cosine has been omitted from the equation). At this point it is easy to obtain the natural frequencies of the system, only the square root of the eigenvalues is required:

$$\omega_i = \sqrt{\omega_i^2} \text{ with } i = 1, \dots, 2N$$

Substituting the variable ω_i into the (1.5) is possible to find the eigenvectors of the system.[4] After implementing of this system on MATLAB it was possible analyse the results. It was used for example a model with $N=146$ sectors. The eigenvectors $\{\psi_i\}$ found, can be divided in two categories related to the nodal diameter. The nodal diameter 0 and $\frac{N}{2}$ are called *stationary* mode shapes that corresponds to the *Umbrella mode*, showed in the figure Fig. 9. In the *Umbrella mode* all the sectors move in the same direction at the same time, the amplitudes however are different. Note that the results are divided in Dofs of Disk and Dofs of blades.

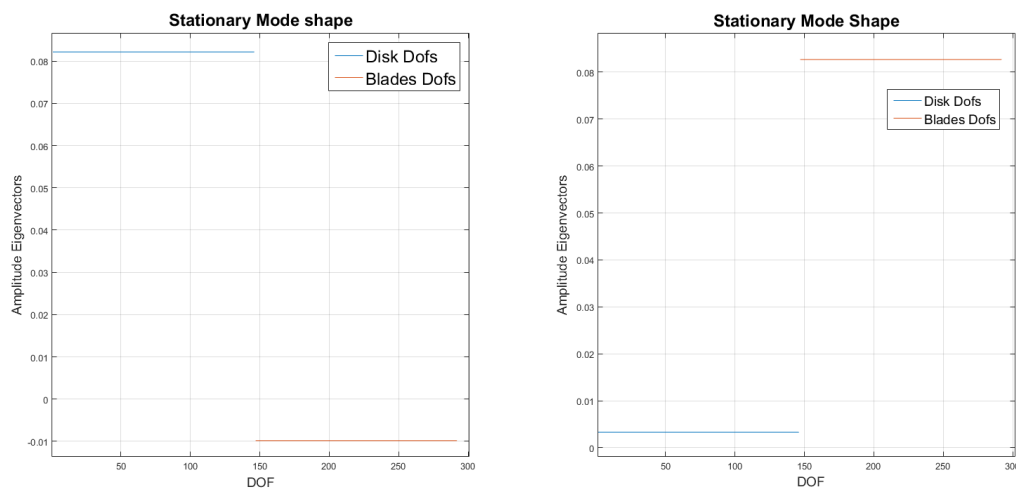


Figure 8: Umbrella mode for $\{\psi_0\}$ on the left and $\{\psi_{N/2}\}$ on the right

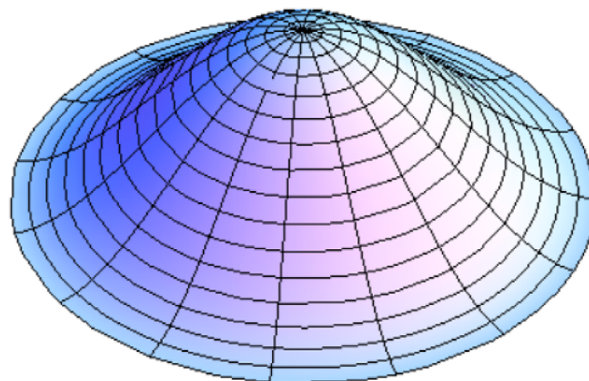


Figure 9: Umbrella mode in 3D [6]

The second type of eigenvectors is *rotating*. They are associated with the couples of natural frequency. The rotation of them is linked to their orthogonal properties expressed through $\sin(n\theta)$ or $\cos(n\theta)$ functions. It is possible to note that the two sinusoids have the same wavelength and the Blades recorded a much higher amplitude values of displacement(eigenvector). This phenomenon is quite physical understandable. In the next figures will be shown two examples of Rotating Mode for the corresponding Mode Shape 1x0 with one nodal diameter and Mode Shape 4x0 with 4 nodal diameters. Both for Disk Dofs and Blade Dofs.

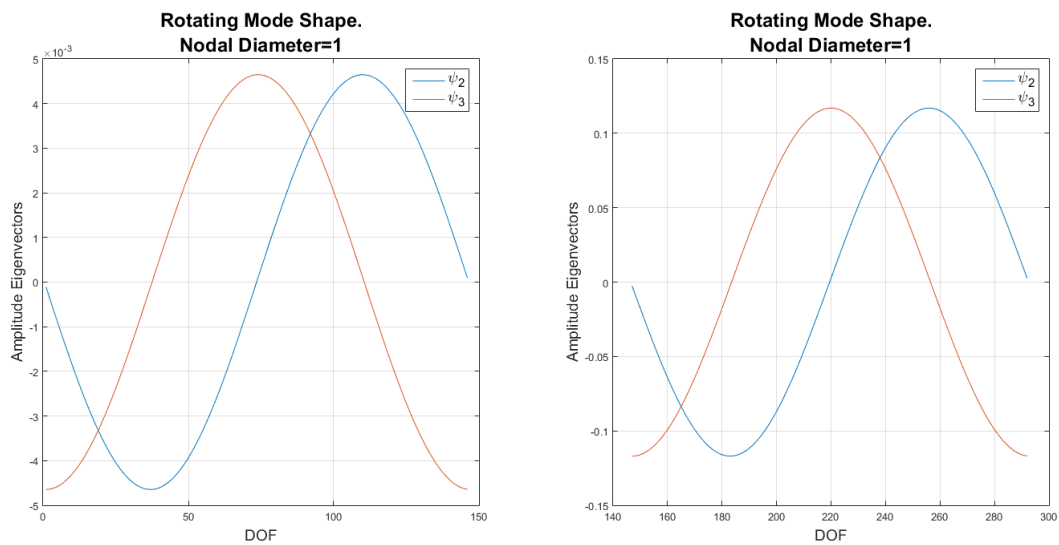


Figure 10: "Disk Dofs" on the left and "Blades Dofs" on the right

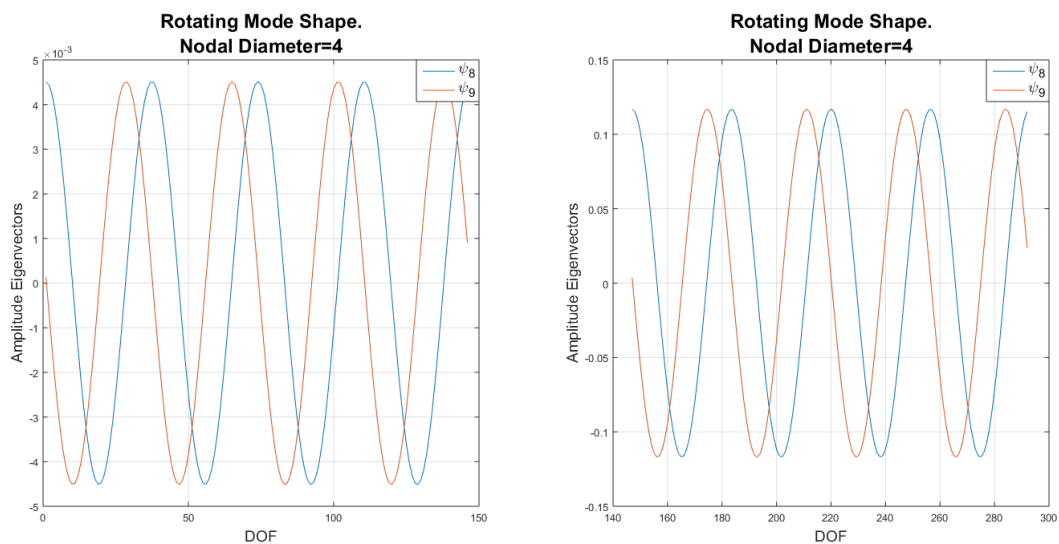


Figure 11: "Disk Dofs" on the left and "Blades Dofs" on the right

1.2 Single Sector

One of the goals of this dynamic analysis of bladed disk is to take advantage of the cyclic symmetry of the structure to obtain much less computer time and storage of calculation. It is possible to do it by considering only one substructure(one sector)and applying appropriate complex constraints at its boundary with the following substructure that has a constant phase difference. Obtaining so a complete analysis of the structure. This method is more convenient more are the number of sectors N [1]. For do this, a new model is proposed on this subsection in order to restrict the dynamic analyses only to the single sector as showed in the following figure:

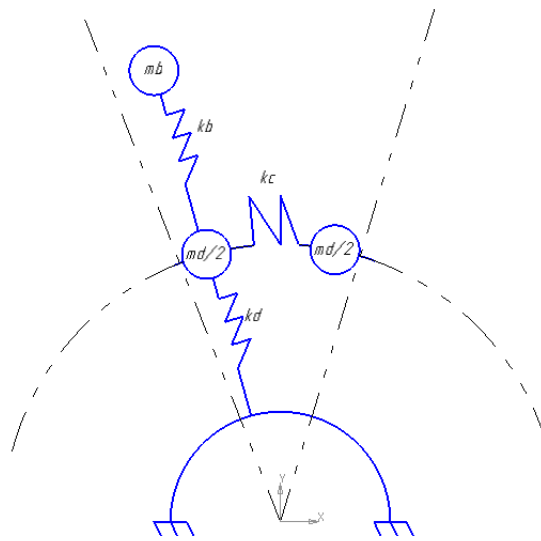


Figure 12: Model of single sector

It is possible to note that, in this case, the mass was split in half in order to respect the cyclic symmetry. This brings also to define a new set of parameters that represents the new model and then impose some constraints for the cyclic symmetry. There is always the mass of the blade m_b and then two times half mass of the disk $\frac{m_d}{2}$. The mass of the blade is linked to one-half mass of the disk through the stiffness element k_b . While k_c links the two half mass of the disk and k_d links half mass of the disk to the ground. So for the cyclic symmetry was imposed:

$$\{x\} = \{x_{d,L}, x_b, x_{d,R}\}^T$$

where $x_{d,L}$ and $x_{d,R}$ are the disk sector Dofs, respectively, of Left and Right position and x_B is the Dof of the Blade. The mathematical variables now are three. The purpose is to find a mathematical relation that lets to reduce to two these variable. At this point is possible to define the dynamic system equation for the substructure without external forces applied that should be:

$$[M_s]\{\ddot{x}\} + [K_s]\{x\} = [0] \quad (1.6)$$

where:

$$[M_s] = \begin{bmatrix} \frac{m_d}{2} & 0 & 0 \\ 0 & m_b & 0 \\ 0 & 0 & \frac{m_d}{2} \end{bmatrix} \quad (1.7)$$

$$[K_s] = \begin{bmatrix} (k_d + k_c + k_b) & -k_b & -k_c \\ -k_b & k_b & 0 \\ -k_c & 0 & k_c \end{bmatrix} \quad (1.8)$$

As in the previous chapter, $[M_s]$ and $[K_s]$ represent, respectively, Mass matrix and Stiffness matrix of the sector. (the subscript s is for sector). In this model, they assume the shape of 3x3 Matrices due to the 3 Dof explained.

In the next step, a boundary condition will be introduced in order to reduce the number of Dof of the new model. This will let to consider also all the other sectors that, as said, are related to the main one through a harmonic function but with a different phase. The difference of phase will be called *inter-blade phase angle* ψ_n . The boundary condition could be, for example, impose that the right Dof is a function of the left one through a parameter linked to ψ_n . It means:

$$\{x_{d,R}\} = e^{i\mu}\{x_{d,L}\} \quad (1.9)$$

Thanks to this condition the number of Dof of the system pass from three to two and the new parameter of the system become:

$$\{x'\} = \{x_{d,R}, x_b\}^T \quad (1.10)$$

To obtain the initial parameter $\{x\}$ it is used a proper transformation matrix T that gives:

$$\{x\} = [T]\{x'\} \quad (1.11)$$

$$[T] = \begin{bmatrix} 1 & 0 \\ 0 & 1 \\ e^{i\mu} & 0 \end{bmatrix} \quad (1.12)$$

With the same procedure of the entire structure is possible to derive two times $\{x\}$ and substitute the results to the (1.6). Then multiply and pre-multiply, respectively, by $[T]$ and by $[T]^T$ the

Mass Matrix $[M_s]$ and the Stiffness Matrix $[K_s]$ obtaining the final system:

$$[M'_s(\mu)]\ddot{x}' + [K'_s(\mu)]x' = 0 \quad (1.13)$$

with $[M'_s(\mu)] = [T]^T[M_s][T]$

and $[K'_s(\mu)] = [T]^T[K_s][T]$

Note that the value of μ can assume both positive or negative values of inter-blade phase angle ψ_n such as:

$$\mu = \pm\psi_n = \pm\frac{2\pi}{N}n;$$

The inter-blade phase angle ψ_n depends on nodal diameters $n = \left[0, \dots, \frac{N}{2}\right]$ with N even number. It was assumed only positive values of ψ_n .

After performing the modal analysis of the system (1.13), two frequencies and a couple of eigenvectors for each sector has been found. They are listed in the modal matrix $[\psi_s(\mu)]_{2 \times 2}$. For example, nodal diameter is equal to 1 should be obtained the same eigenvalues and eigenvectors of the Entire Structure analysis for nodal diameter equal to 1. It's possible to make a mathematical comparison between the two methods by expanding the modal matrix $[\psi_s(\mu)]_{2 \times 2}$ through a matrix of expansion $[T_{\psi_s}]_{2N \times 2}$ that is $2N \times 2$ because expands the study of eigenvectors to all the sectors with two Dof each. The procedure is shown below:

$$[\psi_{exp}(\mu)] = [T_{\psi_s}][\psi_s(\mu)] \quad (1.14)$$

$$[T] = \begin{bmatrix} \dots \\ e^{ik\mu}[I] \\ \dots \end{bmatrix} \quad (1.15)$$

with $[I]$ as 2×2 matrix and $k = [0, \dots, N - 1]$ for each μ .

It's clear that the eigenvalue problem gives complex eigenvectors and any complex mode shape of the structure can be expressed in terms of the deflected shape of just one substructure, by use of the appropriate value of ψ_n .

In the following graphics are showed some example of eigenvectors values obtained thanks to this method about Mode Shape 4:

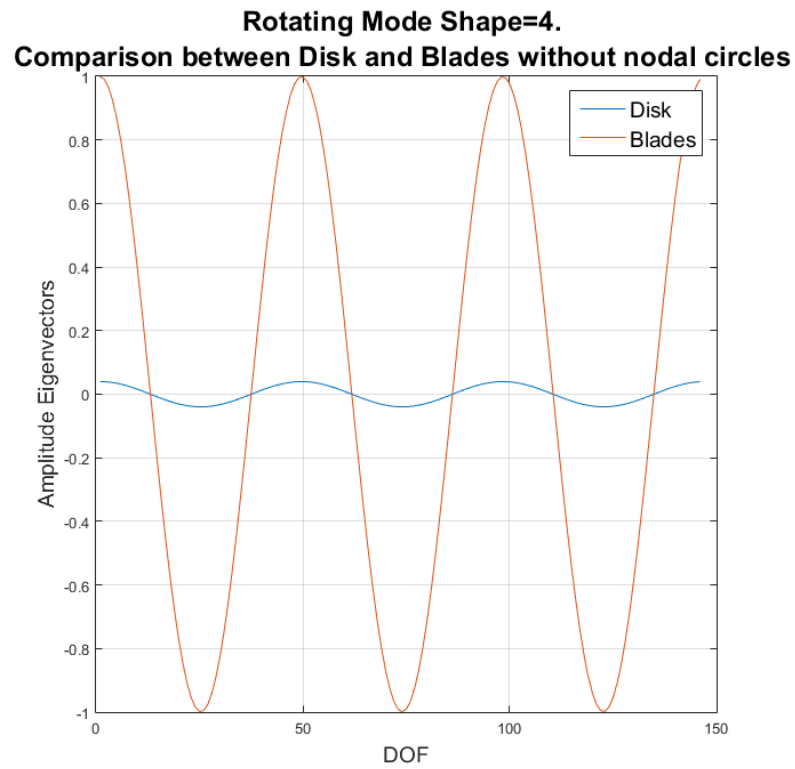


Figure 13: Mode Shape 4x0 without nodal circles

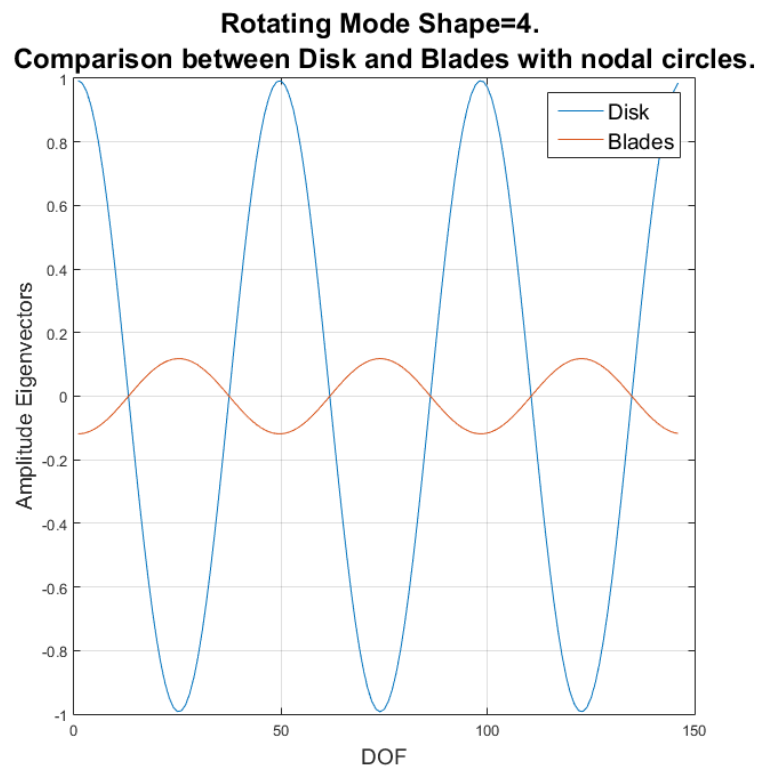


Figure 14: Mode Shape 4x1 with nodal circles

To sum up, it was shown how for a given value of ψ_n , it is possible to evaluate all the corresponding rotating mode shapes of one substructure and thence of the whole structure, from the mass and stiffness matrices of one substructure without any approximation. By repeating this for every possible value of ψ_n , it is possible to obtain all the mode shapes of the complete structure [1].

More are the Dofs of the system, more are the time and storage required from the processor of a computer. This analysis of single substructure with complex constraints demonstrates that time and storage are reduced, especially for those eigenvalues subroutines that take a lot of central processing time(CPU time) once $[K]$ and $[M]$ have been set up. This CPU time is proportional to the number of Dof cubed for this reason reduce the Dof was one of the main purposes of the new system. So it was reduced the starting system of the single sector from three degrees of freedom to two. This method of analysis of rotationally periodic structure is implemented in a lot of modern software like Ansys that has been used for the analysis of the next chapter.

The next chapter will take into account the presence of a Force Response in the general system that lets to analyze the Frequency Response that better represents the real behavior of the Bladed disk. This one, as it will be explained, suffers the presence of a mix of forces more or less strong that generate stresses on the blades and on the disk and they must be considered.

2 Chapter 2

Forced Response Analysis

As explained, during the start procedure and when it is operating, an engine generates several vibration frequencies caused by its rotation. The vibrations are applied to all the elements of the engine and especially on the bladed-disks which composed the compressor and the turbine. It is important to gain an early understanding of the dynamic behaviour of bladed-disk assemblies to prevent extremely dangerous resonant conditions for turbo-machinery stages. Even if, at present, bladed-disk vibrations are not involved in any incidents, turbo-machine failures show the necessity to predict them. The stress on the bladed disk born due to forces that act on from the airflow to the blade adding on the rotational speed.

When an engine rotates, it emits a response(vibration) at a certain amplitude. As the speed of rotation changes, the response changes too. The relation between this response, the rotational speed and the frequency of rotation are expressed by a new parameter called *Engine Order* (EO). In general, it aids in the analysis of noise and vibration signals in rotating machinery. In this case, it will be useful to understand how blade or disk contributes to the overall level of vibration. So the EO excitation is a periodic force. The sources of excitation could be self-excitation or flutter, general unsteadiness and random turbulence or non-uniformities in working fluid pressure. Angular non-uniformity in pressure causes dynamic excitation of rotating blades at frequencies that are multiples of the rotation speed and with spatial distributions that match nodal diameter modes.[7]

The frequency f_i of the harmonics at which the engine is operating depends on the speed turbine:

$$f_i = \frac{EO * \Omega}{60} \quad (2.1)$$

where Ω is the rotational speed (rpm).

With the variation of the rotation speed, is possible to draw for each value of EO the n^{th} EO line.

If the time and revolutions can be related to a rotating system, then the same phenomenon can be expressed as either a frequency or an order. Thus knowing the revolutions per minute (rpm) of a rotating system allows frequency and order to be related to each other.

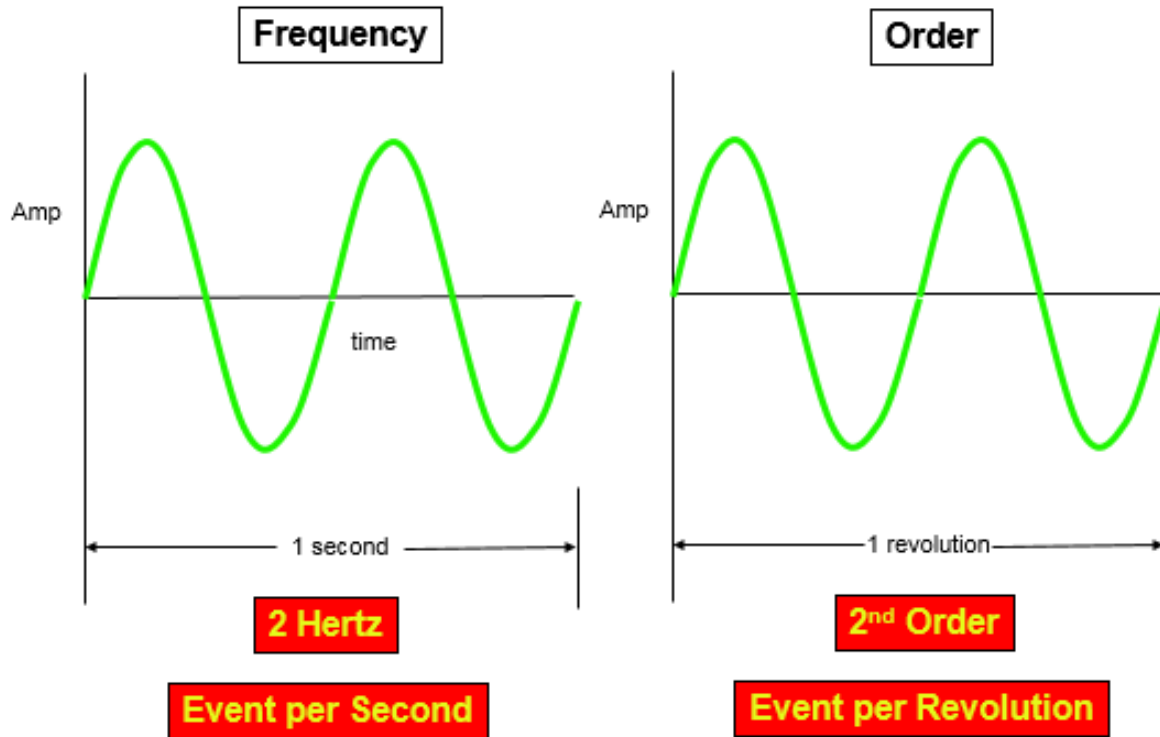


Figure 15: Frequency and Engine Order comparison

Note that for bladed-disk assemblies only certain engine orders can be excited. These are defined as:

$$EO_{\alpha,ND,p} = \alpha N + ND \quad (2.2)$$

where:

– $\alpha = 0, 1, 2, \dots, N$

– p corresponds to the sign “+” or “-”.

– ND corresponds to the number of nodal diameters

Example: $EO_{5,4,-} = 5N - 4$.

After this dissertation about what is the Engine Order is time to analyze the Force that acts on the engine. This force is showed as axial in the following pictures but from theory is known that its direction is arbitrary because it has a component in all three direction axial, radial and tangential. For this step of analysis is not important the direction but just the meaning of this force and how to use it for the calculation of frequency response in the 2D model that was created.

The excitation force vector $\{F\}$ that acts on the blade is shown below:

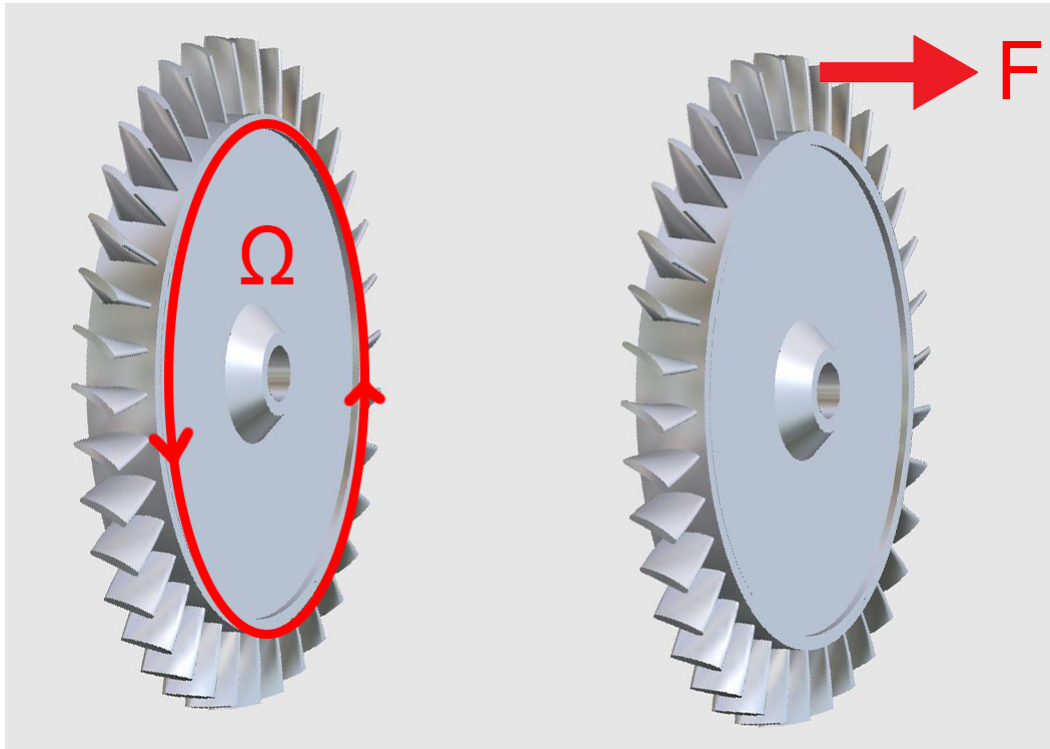


Figure 16: Excitation Force

It can be expressed as a harmonic function:

$$F = \{\overline{F_0}\}e^{(i\omega t)} \quad (2.3)$$

This function has ω as excitation frequency and $\{\overline{F_0}\}$ as amplitude. This amplitude results in a complex value due to the relation with the inter-blade phase angle and the position of the blade m .

$$\{\overline{F_0}\} = \{F_0\}e^{(i\psi m)} \quad (2.4)$$

where

- $\{F_0\}$ amplitude vector of forcing function ($F_0 \in R$)
- ψ inter-blade phase angle ($\psi = \frac{2\pi}{N}n$)
- m position of the blade ($m = 1, \dots, N$)

After the definition of Force Excitation is possible to define the system of equation for both models of the Entire Structure and Single Sector as it was done in the previous chapter.

2.1 Entire Structure

For the entire structure, the presence of External Force brings to a new parameter that should be considered in the main equation of the model such as a damping matrix $[C]$. as known, Damping is the dissipation of energy from a vibrating structure. From the theory, it is known that the dissipation is the transformation of the energy into the other form of energy and this means that there is a removal of energy from the vibrating system. The type of energy into which the mechanical energy is transformed is dependent on the physical mechanism that causes the dissipation. In the most common case, this energy is converted into heat. It is true also for the compressor's rotor wheel.

It is correct to say that any mathematical representation of the physical damping mechanism in the equations of motion of the vibrating system has a generalization and approximation and generalization of the true physical situation because the specific ways in which energy is dissipated in vibration are depended upon the mechanism that acts on the structure. It means that the type of damping that is present in the structure depends on the predominant mechanism in each situation. For example, the Flight Phase could affect the operating condition.[5]

The main equation of the system should be:

$$[M]\{\ddot{x}\} + [C]\{\dot{x}\} + [K]\{x\} = \{F\} \quad (2.5)$$

It was assumed that the damping phenomena has only viscous nature even if any causal model which makes the energy dissipation functional non-negative is a possible candidate for a damping model. To obtain the modal damping matrix it is necessary pre-multiply and post-multiply the modal damping matrix $[c_r]$ by, respectively, the inverse of transpose modal matrix $([\Psi]^T)^{-1}$ and the inverse of the modal matrix $[\Psi]^{-1}$:

$$[C] = ([\Psi]^T)^{-1}[c_r][\Psi]^{-1} \quad (2.6)$$

For the definition of $[c_r]$ is necessary to establish a modal damping ratio ζ_r for each mode. To be clear, the damping ratio is a dimensionless measure describing how oscillations in a system decay after a disturbance. It depends from:

$$[c_r] = \text{diag}(2\zeta_r \sqrt{k_r m_r})$$

Is it clear that in the main equation the matrix $[M]$ and $[K]$ are now modal matrix obtained also by pre-multiply and post-multiply, respectively, with the inverse of transpose modal matrix $([\Psi]^T)^{-1}$ and the inverse of the modal matrix $[\Psi]^{-1}$. So the value of k_r and m_r corresponds to

the diagonal of respective modal mass and stiffness matrix.

Analyzing the differential equation, the solution obtained is a harmonic function as:

$$\{x\} = \{X_0\}e^{(i\omega t)} \quad (2.7)$$

Taking the derivatives of $\{x\}$ and substituting into (2.5) is possible to derive the value of Response Amplitude $\{X_0\}$ as:

$$\{X_0\} = [K_{dyn}]^{-1}\{\bar{F}_0\} \quad (2.8)$$

The dynamic stiffness matrix $\{K_{dyn}\}$ in the formula corresponds to:

$$[K_{dyn}] = [K] - \omega^2[M] + i\omega[C]$$

This matrix is a $2N \times 2N$ matrix. Each solution of the system is listed for different Engine Order. It is showed now an example of Force Response for the second nodal diameter that is present for a range of frequency around the value of $f = 98$ for a system with $N=146$ sectors and a modal damping ratio of 0.005.

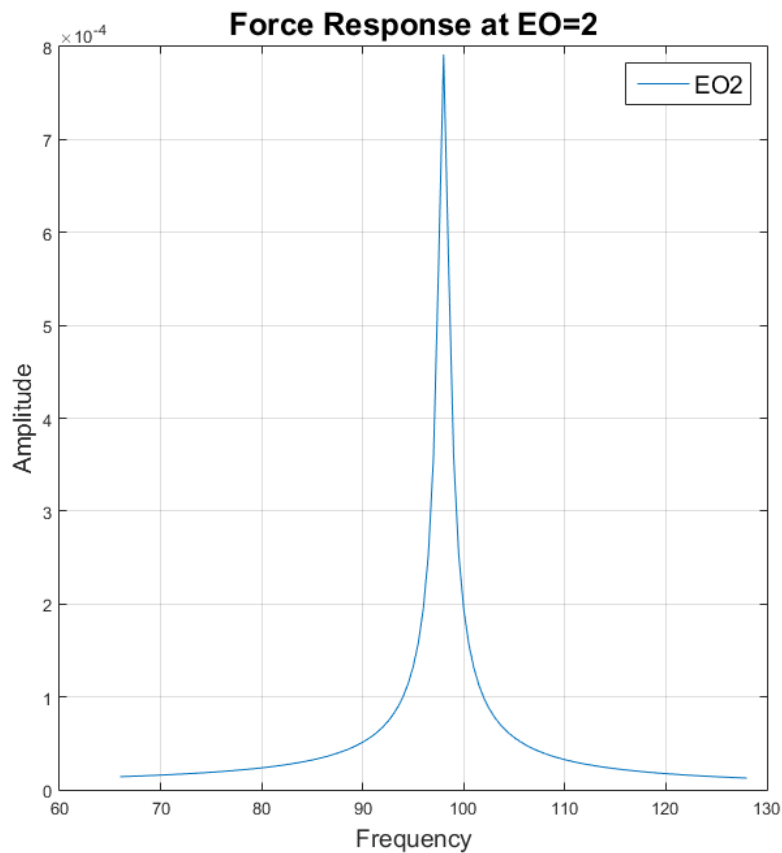


Figure 17: Example of Force Response with EO=2 for disk

Another Example that could be done, concerns the variation of modal damping ratio. It is expected that more is the damping force acting on the system, less should be the force response. It was demonstrated in the following picture where it's clear how the amplitude of the force became fainter. This example is always related to the second Mode Shape.

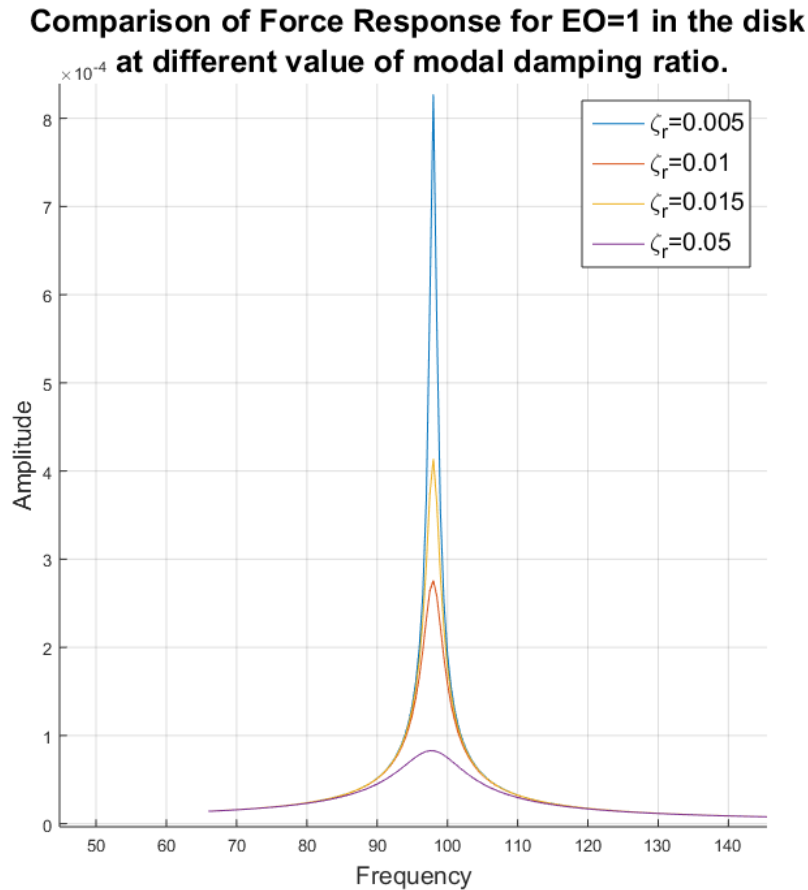


Figure 18: Example of Force Response for EO=1 for disk with different Modal Damping Ratio/

When the structure is excited by a frequency that concerns the disk, it doesn't mean that the blade doesn't feel this Change. Even the blade will have a little response from that frequency that excites the disk, as results of a resonance phenomenon. In general, this influence is neglectable because very small. It's curious to note that this small response is different for disk and blade cases. Analyzing the small blade resonance, it has just the same shape as the general one with a peak of amplitude in the center. While for the small resonance of the disk it as an unusual shape with a reverse amplitude that indicates that the disk vibrates in two opposite directions under the blade's frequency excitation. This due do the born of the nodal circle at higher frequencies. The two cases are shown below and in addition, there is a zoomed figure of the small disk response to note the reverse direction of the amplitude.

This phenomena is showed in the following figures:

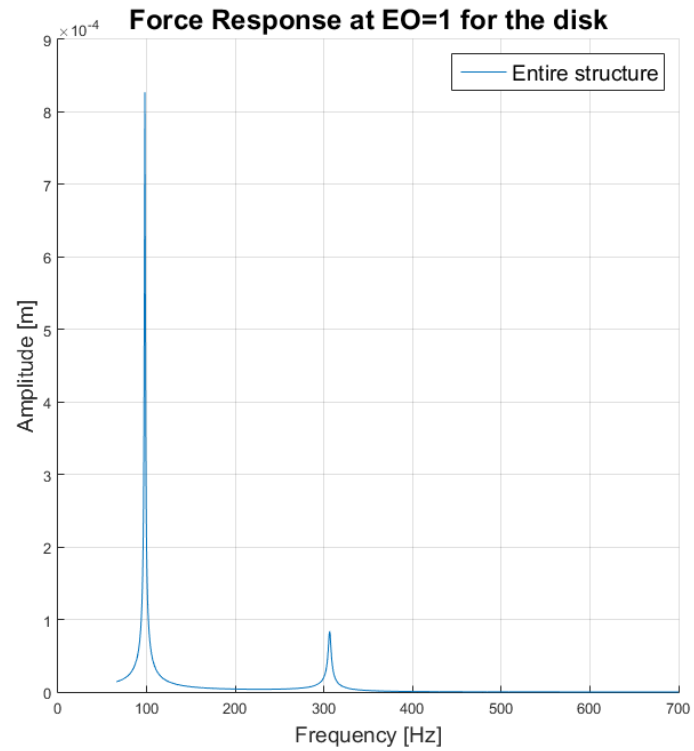


Figure 19: Example of Force Response for EO=1 for Disk.

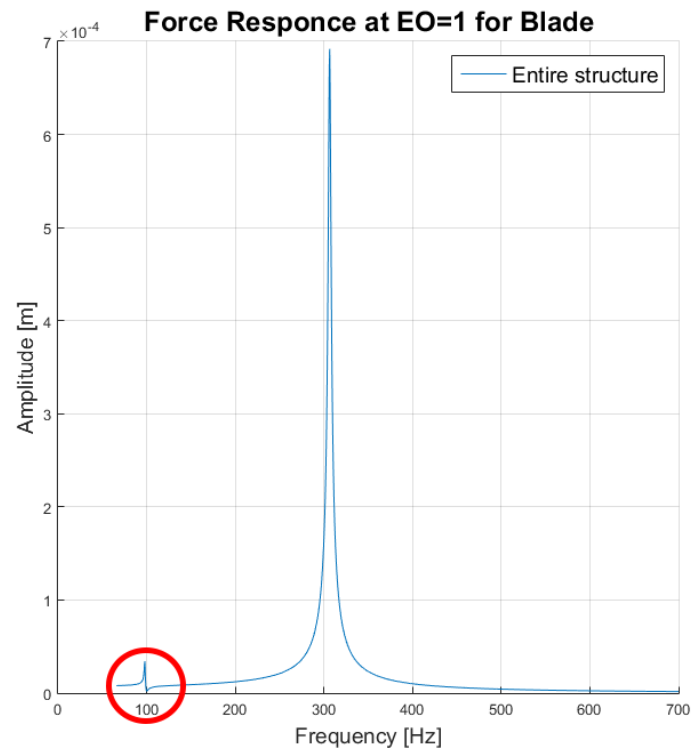


Figure 20: Example of Force Response for EO=1 for Blade.

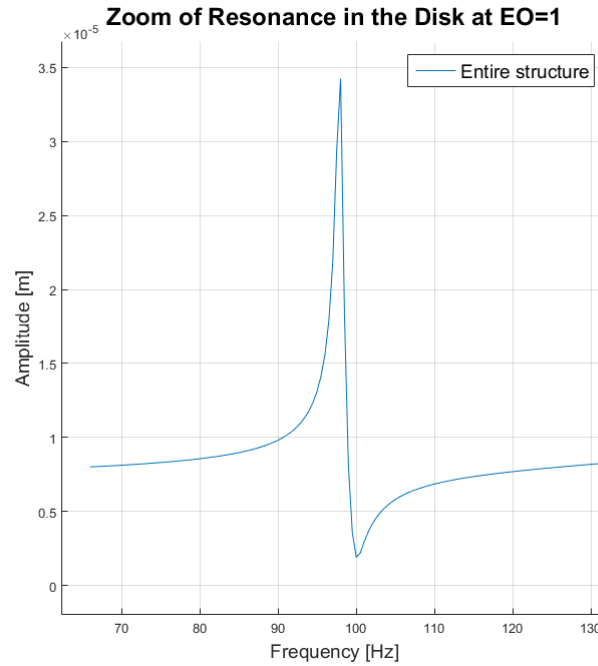


Figure 21: Zoom of Resonance in the Disk at EO=1.

Higher is the EO, lower should be the amplitude of this small resonance in the other element that not concerns that frequency range studied. This is true until the reaching of EO=73 that is half of the number of sectors. And the same rule is valid for the Blade Dof for which this value is EO=219. The figures will make clear this rule:

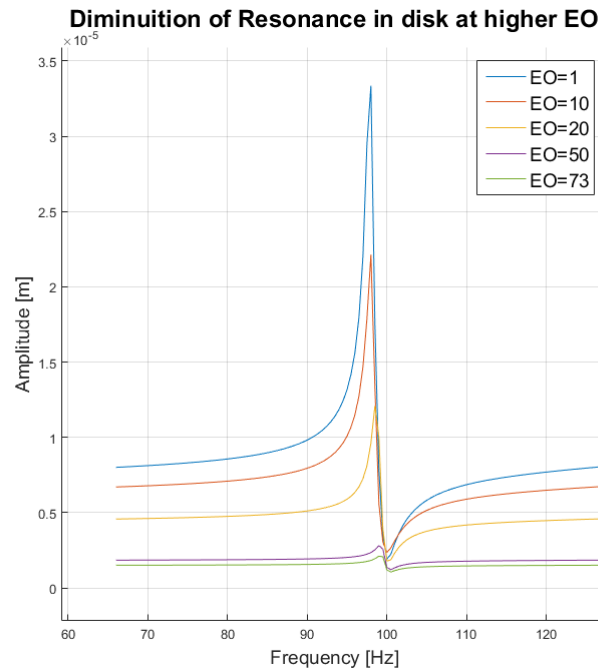


Figure 22: Diminution of Resonance in the Disk at different EO.

This happened only because the structure is symmetrical.

As explained the Engine Order determines the relationship between the response of the engine at a certain rotational speed. So an analysis of the Force response to different values of Engine Order lets to understand better the contributes of Blade and disk to the overall vibration that affects the rotating engine. As an example is showed the case of the Force Response of the blade at different EO for the First Mode Shape with a nodal circle too.

Comparison of Force Response of the blade at different EO

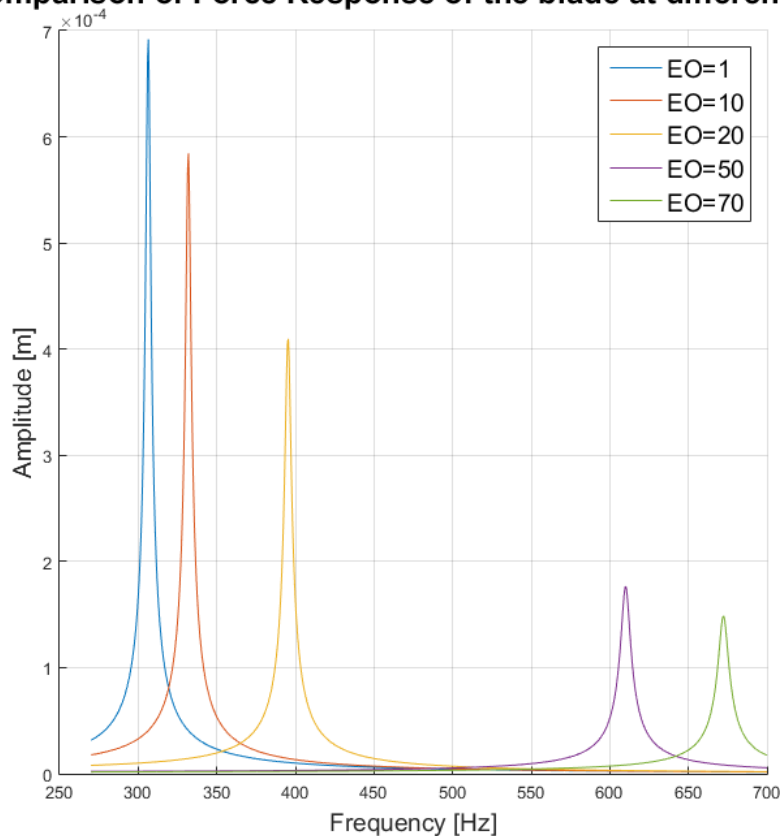


Figure 23: Force Response at different EO.

In this case, higher is the EO value and lower is the amplitude of the Force Response. This is not a general rule and depends form different factors such as, for example, the number of sectors of the structure. The next subsection will be showed the study of how is possible to use the cyclic symmetry of the structure to success in the dynamic analysis of the overall structure just studying the single sector.

2.2 Single Sector

It is possible to apply the theory of Thomas even with a Force Response system thanks to the cyclic symmetry of the structure. So the number of Dof will decrease. It will pass from three to free, like for Chapter 1, due to the boundary condition that links the right side with the left one.

$$\{x'\} = \{x_{d,R}, x_b\}^T \quad (2.9)$$

The excitation force will be applied on the Dof of the blade and is:

$$\{F_{0s}\} = \{0, F_0\}^T \quad (2.10)$$

The presence of the excitation force introduces in the main equation of the system the damping matrix that is possible to obtain in the same way of the Entire Structure.

$$[M'_s(\mu)]\ddot{x}' + [C'_s(\mu)]\dot{x}' + [K'_s(\mu)]x' = \{F_{0s}\}^{(i\omega t)} \quad (2.11)$$

To confirm the value of this method is possible to compare the two ones in the following graph:

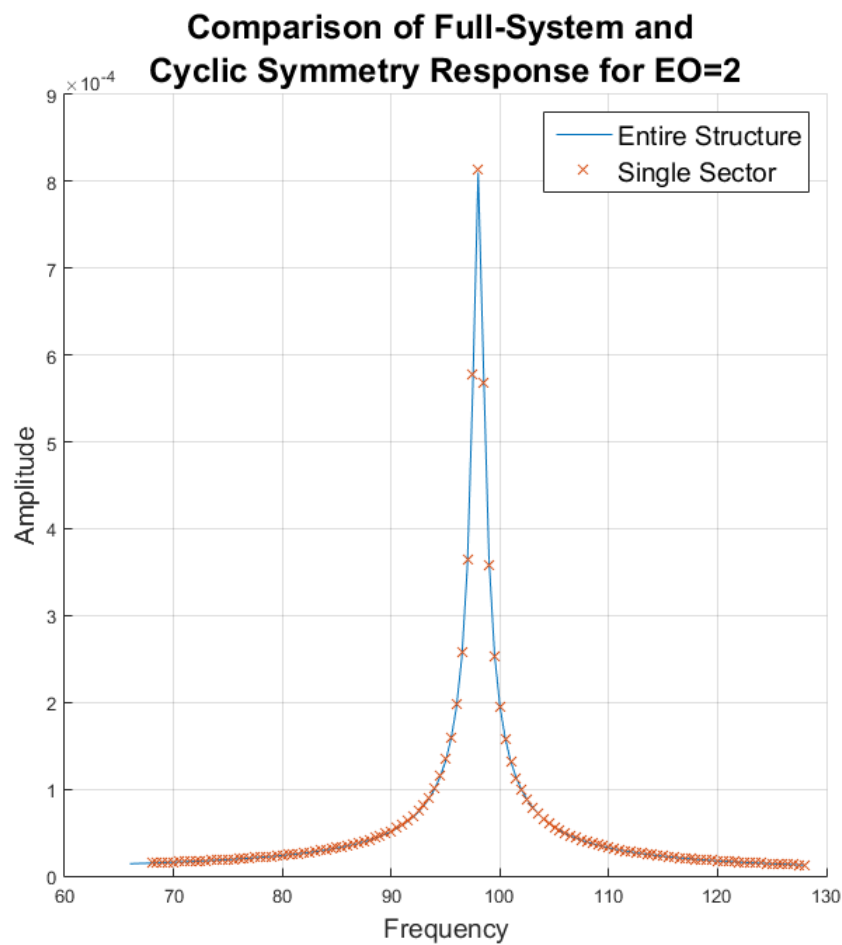


Figure 24: Comparison of Full-System and Cyclic Symmetry Response for EO=2

3 Chapter 3

Mistuning Analysis

The present chapter will introduce the concept of mistuning on a bladed disk. After the short introduction of the basic concepts, a simplified model will be analyzed to which a mistuning condition will be simulated. After this process comparison between the 2D and 3D calculation will be done in order to confirm that the method works and to expand the study to a more complex model nearer to reality. To predict correctly the random phenomena of the mistuning should need hundreds of degrees of freedom that will make the computational process very long. The goal of this chapter is also to try to reduce this number applying the mistuning to a model with a lumped degree of freedom applied in the main point that will be discussed later.

3.1 What is the Mistuning?

As several times said, the compressor is a periodic structure consisting of a finite number of identical substructures or sectors that create the closed circular shape. It was demonstrated that it is possible to study only one sector in order to represent the whole bladed disk dynamics by applying the cyclic symmetry constraint at the sector interfaces. After expanding the results performed for the single sector to the whole structure, as a result it is possible to obtain a calculation thanks to what it's showed the amplitude at which each sector vibrates. But as the sectors are all equals even the results are perfectly in concordance. This is not true in reality. There are small differences between sectors that destroys the cyclic symmetry of the bladed disk. This fact let to an unpredictable force response of the structure of the system where such a blade, for example, can vibrate with a larger amplitude than the nominal one. This random disorder affecting the structure is called Mistuning. [9]

The reasons that let Mistuning to appear are several.

- The material with which the blades are build could have a nanostructure that presents some irregularities very difficult to find.
- There could be the possibility that during the assembling of the engine some wrong steps let to an asymmetric final product.
- The asymmetry could also occur after a long time due to aging or due to wear especially in that part of contact condition such as blade root joint, snubbers, shrouds, under platform dumpers.

- The Maintenance or repair process could be dangerous in this case because could introduce new elements that need to interfaces with the old one that could be changed their integrity during their life-time.
- There could be the possibility of Foreign Object Damage.

The mistuning study began in the 1960s when researches like Tobias and Arnolds, Whitehead [2] and Ewins [3] started to study the physics of the mistuning phenomenon. Their studies laid the foundations for the next generation of analysis. They tried to find a solution to avoid the negative effect that a phenomenon of vibration has in the structure of the bladed disk. Their studies where mainly concerned about the forced response analysis of the system in order to catch information about structural stability. Different scientist started to change the point of view of the treatment staying on focus on the aerodynamics aspects for turbo-machinery applications like for example flutter or buffeting that generate instability on the structure. Even if Technology got increasingly sophisticated, the main problems related to the mistuning properties remained unsolved until the 1990s. In these years, different approaches were used in order to better understand the behavior of this phenomenon. One of these approaches was the use of lumped parameters model that let to reduce considerably the number of degrees of freedom of the system and so to make easy the test of the analysis. Crossed to this concept, the “Reduced-Order Models” method grew up thanks to personalities like Yang and Griffin, Wang and Ewins. More recently, Chan and Ewins studied the probability of extreme vibration levels due to mistuning. However, due to differences of the built dynamics model and the adopted analysis methods, there is no solid consensus about the maximum mistuning amplification factor. Furthermore, it is important to note that the adopted analysis methods rely on different assumptions, based on these assumptions, which may further limit their usefulness.[10]

3.2 Simplified model

To start the analysis of mistuning it was created a simplified model on which the experimentation was executed. This step was done due to simplifying the time of calculation of computer and if the mistuning method will work for a simplified model, it will be possible to expand the procedure also for a more complex model. The 3D simplified model was created on Ansys-Workbench Software.

This model represents a Blisk such us a blade and a sector of disk together but it is an analysis that could be expanded to other types of structure. In total, the sectors are 24 so the opening angle of the sector is about 15 degrees. The height of the blade is more or less one-third of the height of the sector. The main goal is to study a way to apply the mistuning so the detail in the shape of the model in this step is not so crucial. It is enough that it simulates a bladed disk.

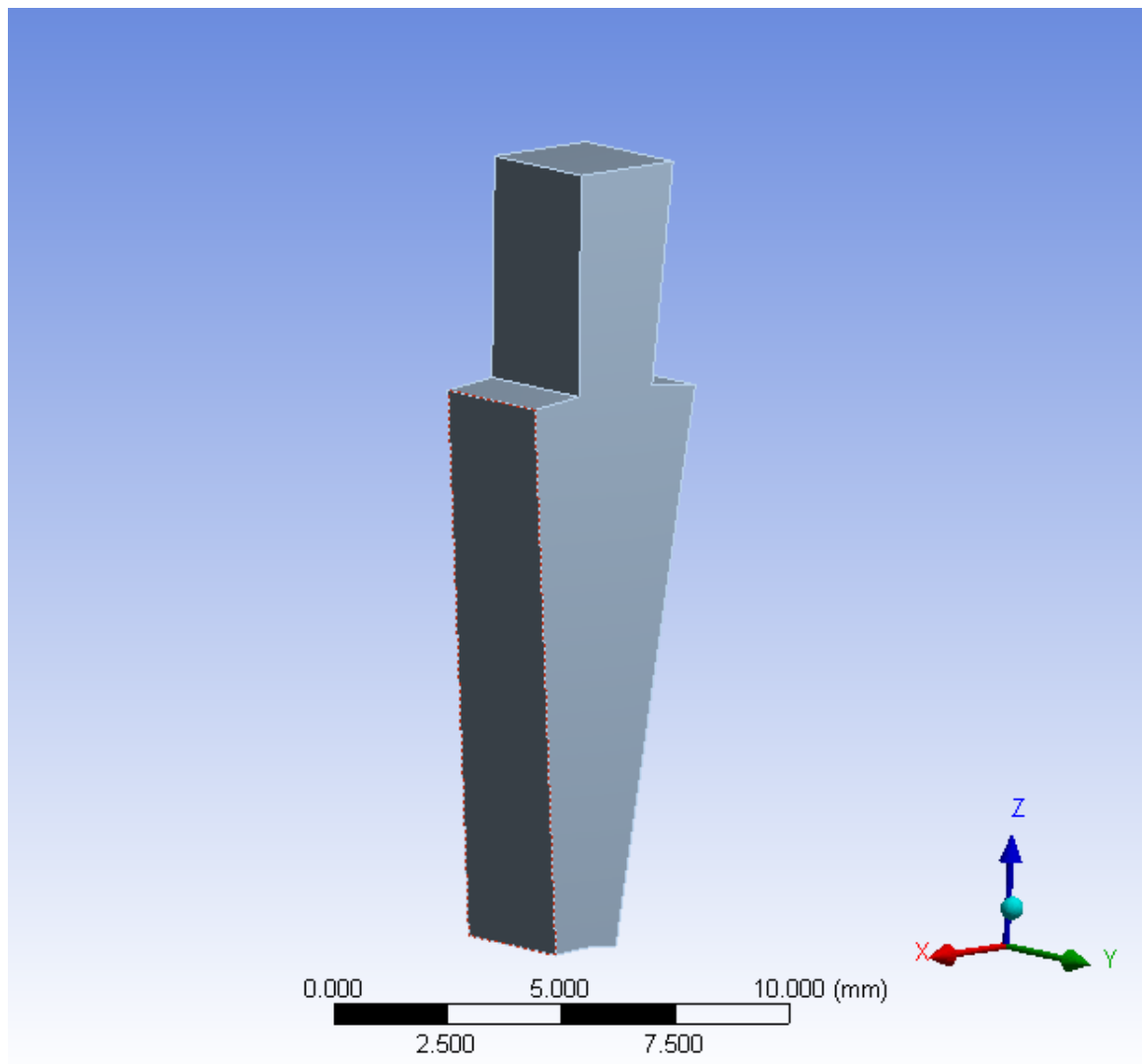


Figure 25: The Simplified Model for the analysis

In order to define the nodes of the FEM Analysis, a coarse Mesh was created. A little number of nodes will help the software on the generation of Matrix K and M. In this case, it was on focus the number of nodes in the interfaces between each sector because it is there that the components will be defined. After this step, a dynamic analysis is done on the 3D model obtaining some frequencies that will be discussed later. Once that the nodes are defined, it was imported the model on the Mechanical APDL platform where a reduced model will be created. It means that from all the nodes only some of them will be taken into account.

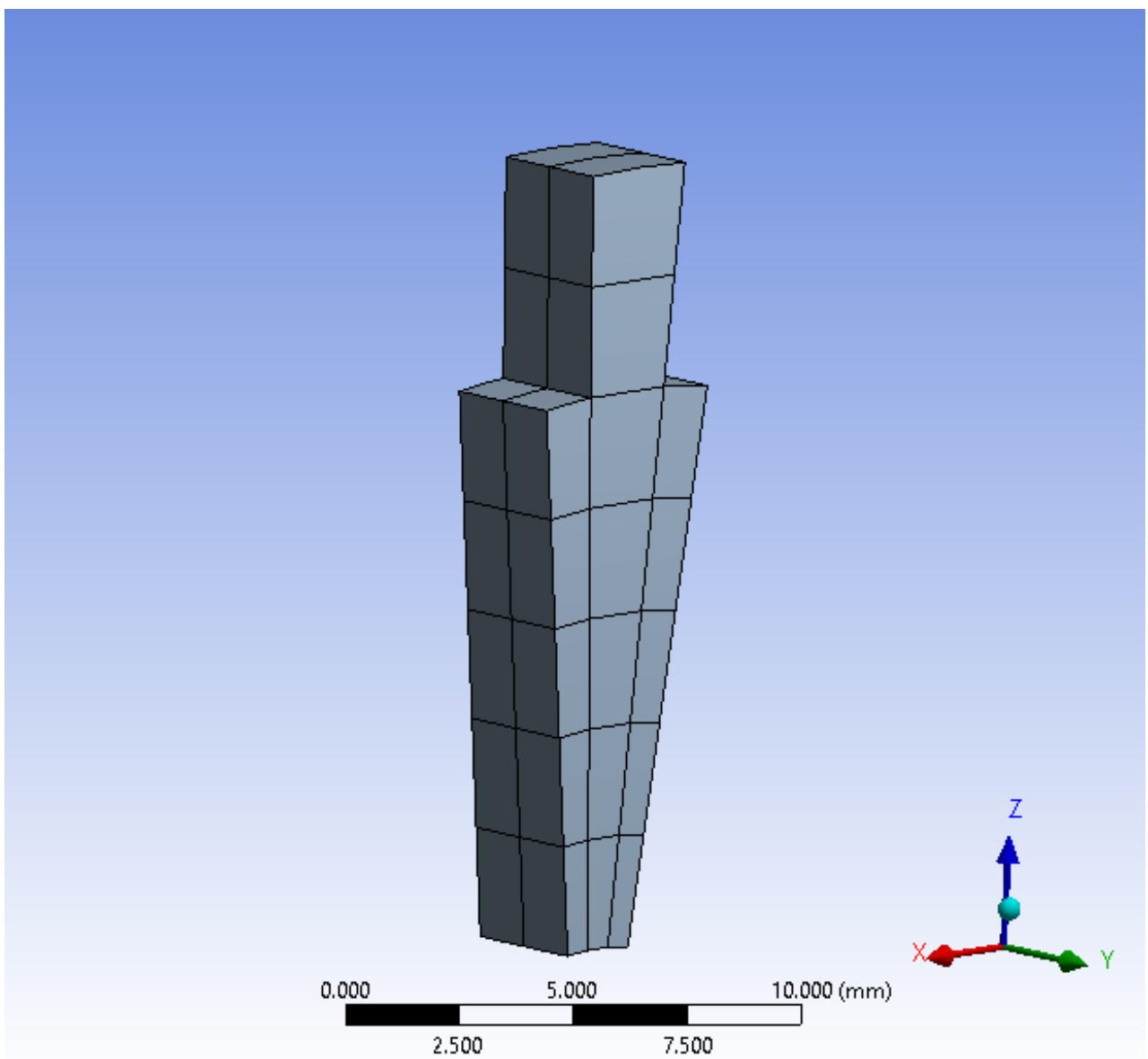


Figure 26: Mesh of the Simplified Model

To Start the modal analysis it is needed to have the matrices M and K. To get them a lumped component was defined on the simplified model. To be exactly 4 components were created. Two of them represent the two interface surfaces right and left of the sector of the disk. They took around 45 nodes. And the other two represent the point of force applying (on the right) and the point of Force Response (on the left) that took only one node. Some routines on Matlab were used to get the matrices M and K. This lets to start the modal analysis on Matlab, such as on the 1D reduced model. Some frequencies were obtained. It is interesting to compare the results from the 3D simplified model on Ansys and the results from the 1D reduced model on Matlab. As a sample, the first 25 frequencies have been compared.

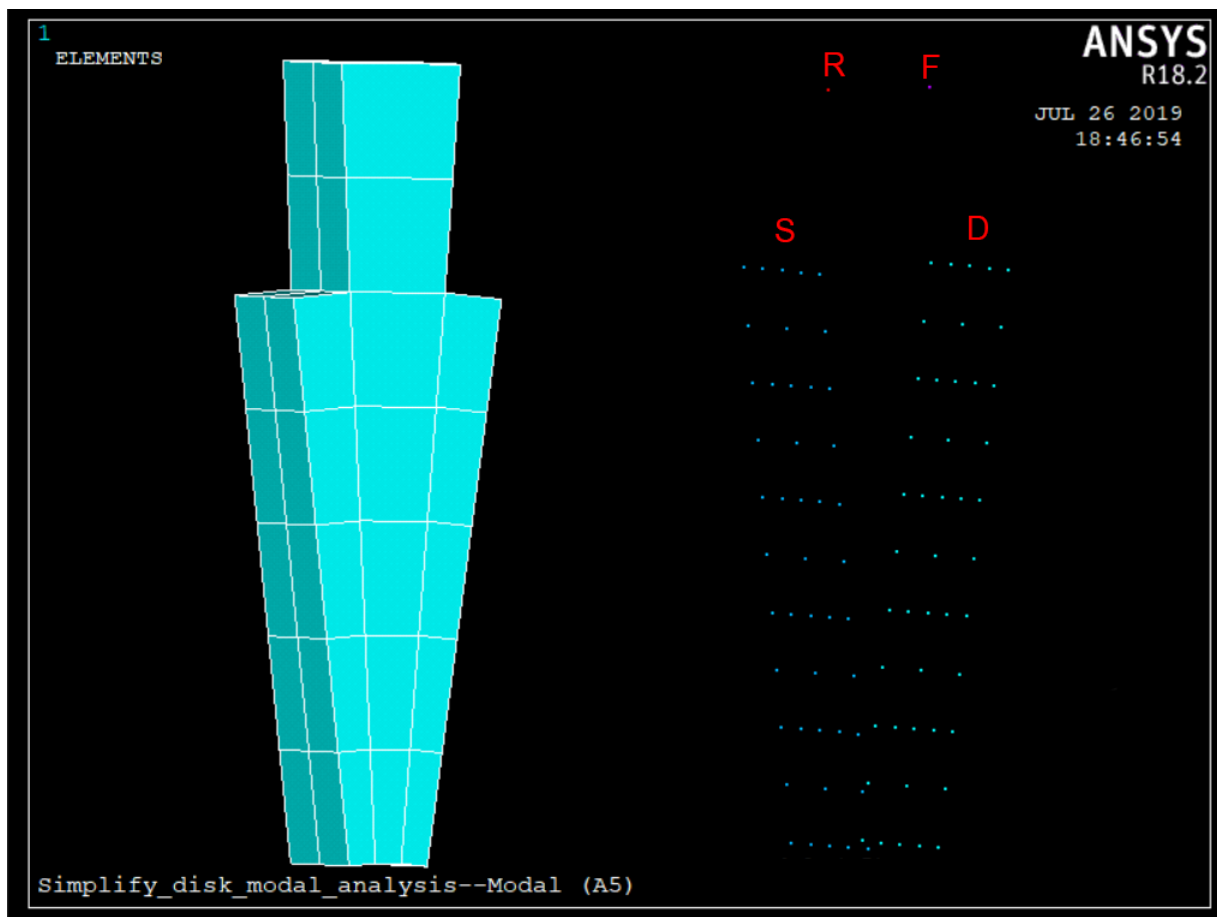


Figure 27: Definition of Lumped Component

	3D Model	1D Model	Error %
1	0	0	0
2	0	0	0
3	0	0	0
4	0	0	0
5	0	0	0
6	0	0	0
7	1394.82	1395.16528	0.00025
8	1872.16	1873.20679	0.0056
9	3190.11	3195.29184	0.00163
10	3221.10	3228.65387	0.00235
11	3535.74	3548.96097	0.00374
12	4710.53	4724.75905	0.00302
13	5069.76	5080.10419	0.00204
14	5694.31	5715.84849	0.00378
15	6305.58	6370.02887	0.01022
16	7164.46	7304.22894	0.01951
17	7955.97	8017.16444	0.00769
18	8457.51	8526.79711	0.00819
19	9097.56	9279.9884	0.02005
20	10368.16	10819.2903	0.04351
21	10673.64	10899.2959	0.02114
22	11195.10	11598.2542	0.03601
23	12677.57	12839.037	0.01274
24	12848.97	13394.8074	0.04248
25	12896.4	13440.186	0.04217

From a general overview is possible to say that the frequencies are almost the same. The 1D Model follows the augmentation of the frequencies in a divergent way. It starts from the first six frequencies that are zero. From the 7th frequency, some difference starts to be present and is monitored through the calculation of the percentage error showed in the third column of the table. It grows up but the value that it reaches is neglectable because too small. This error is easy to understand because in the passage from the 3D model to the 1D model some properties of the Structure have been lost.

The main purpose is to create again the complete structure with all 24 sectors liked. To do it was implemented a Matlab script in which one is able to match the stiffness and mass matrix of every single sector. To start two-sector were matched as showed in the figure. It will be monitored the trend of errors between the 3D and 1D model to better understand if the procedure is correct or not. It is fundamental that the nodes of the interfaces of the right of the first sector matched exactly with the nodes of the interfaces of the left of the second sector.

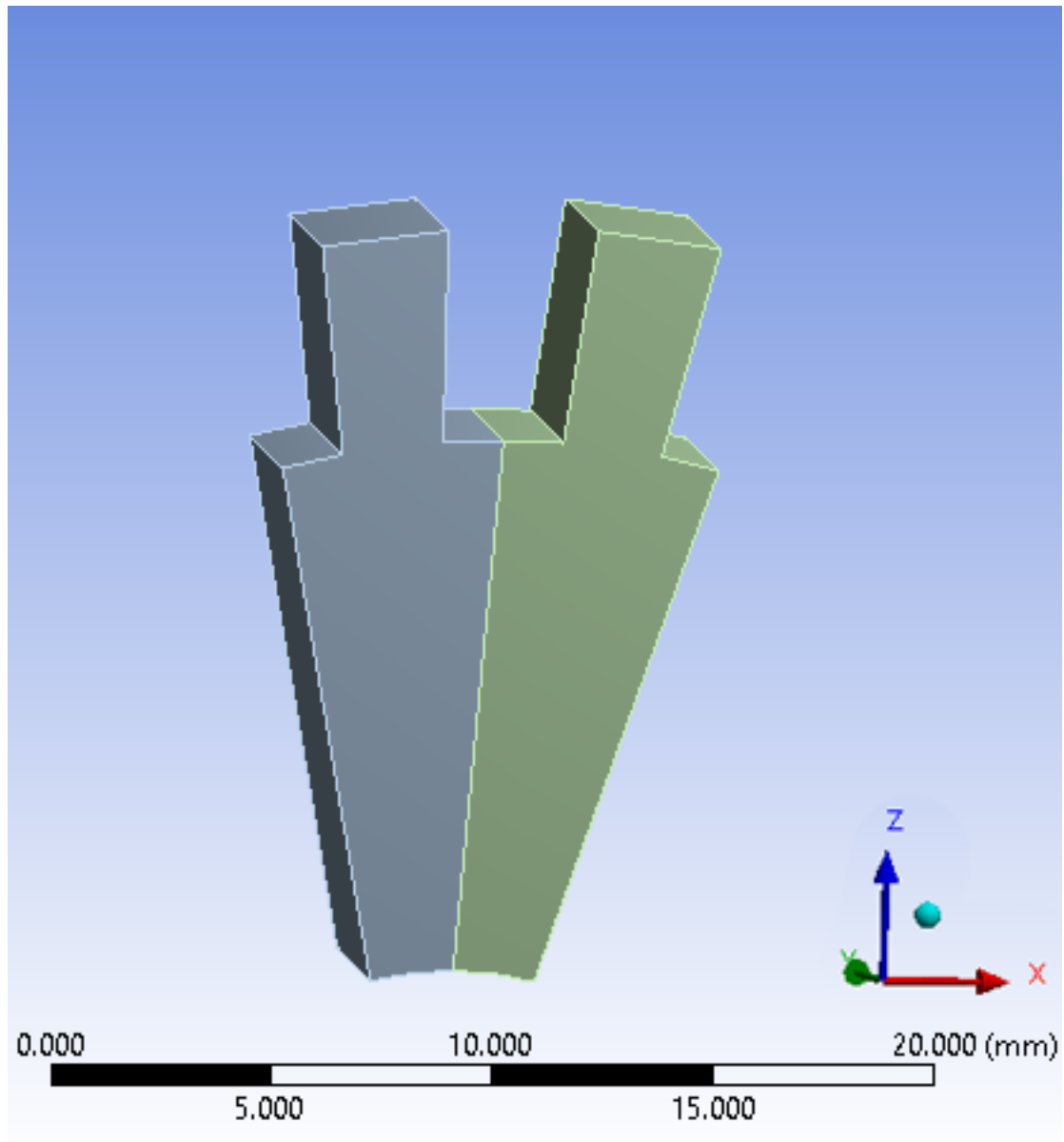


Figure 28: two sectors

	3D Model	1D Model	Error %
1	0	0	0
2	0	0	0
3	0	0	0
4	0	0	0
5	0	0	0
6	0	0	0
7	1218.65	1219.564	0.00075252
8	1404.02	1404.46238	0.00031532
9	1526.43	1529.08774	0.00152945
10	2191.65	2195.00017	0.00174021
11	2773.60	2776.98575	0.00121994
12	3181.57	3184.91957	0.00105357
13	3212.51	3219.13541	0.00175162
14	3999.02	4003.25378	0.00105962
15	4006.29	4017.1678	0.00271529
16	4978.69	4988.99897	0.00207063
17	5145.66	5166.90871	0.00412979
18	5273.73	5311.64616	0.00718954
19	5374.61	5396.83792	0.00413627
20	5817.96	5843.38315	0.00437004
21	5995.05	6013.64018	0.00310159
22	6895.98	6938.47991	0.00616316
23	7503.77	7597.59344	0.01250369
24	8012.9	8112.72847	0.01245906
25	8256.71	8334.81523	0.00945998

Looking to the third column is possible to see that the error is decreasing respect of the table for the single sector. It is expected that the 1D model presents more consistency in results matching two or more sectors. It will be shown just for more comprehension in the case of three and twenty-three sectors and how the error will change.

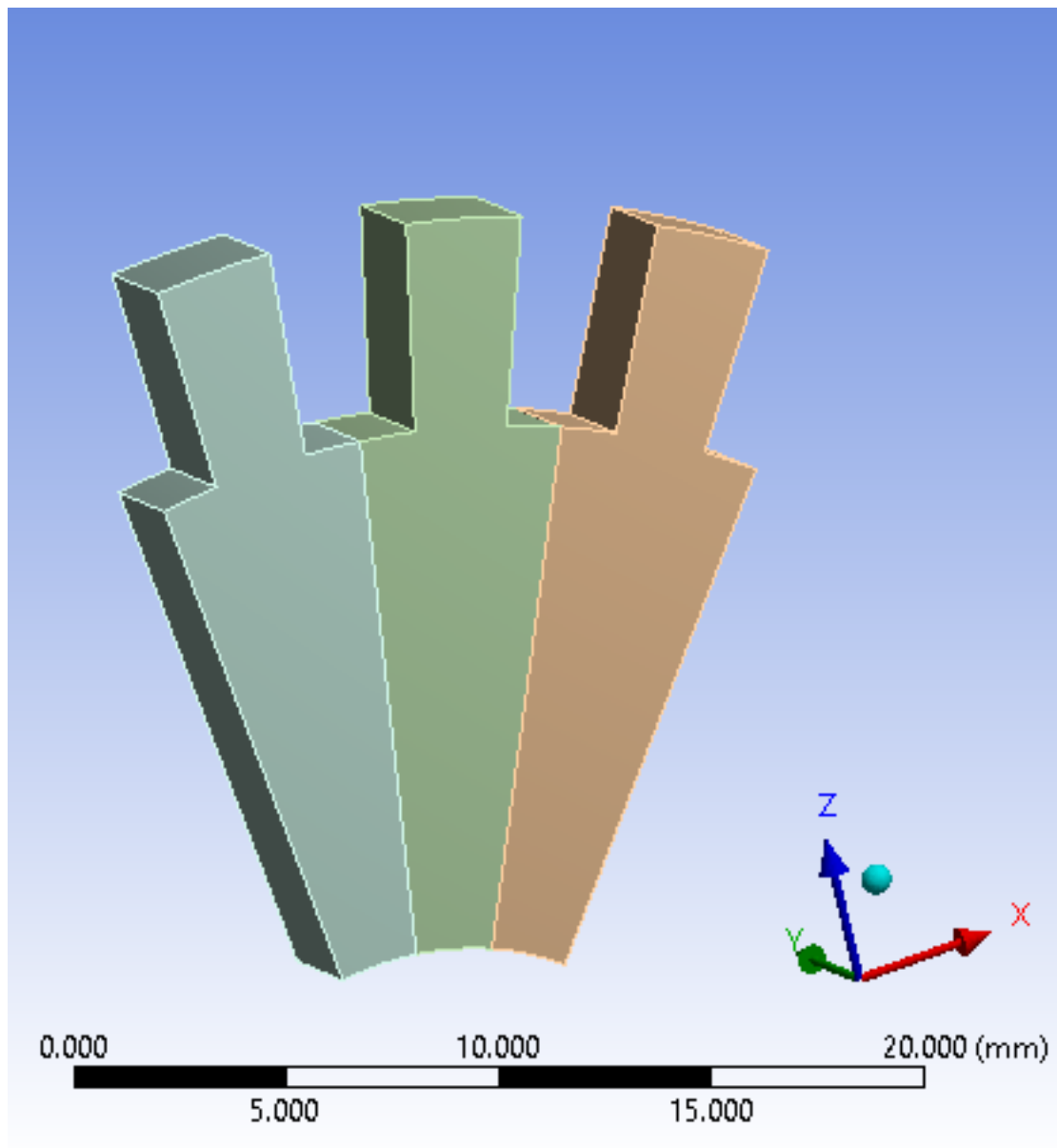


Figure 29: three sectors

	3D Model	1D Model	Error %
1	0.00	0.00	0.00
2	0.00	0.00	0.00
3	0.00	0.00	0.00
4	0.00	0.00	0.00
5	0.00	0.00	0.00
6	0.00	0.00	0.00
7	1040.58	1041.243165	0.00063818
8	1050.22	1051.109471	0.00084309
9	1422.93	1423.499289	0.00040003
10	1473.65	1475.89823	0.00152357
11	1577.66	1581.518303	0.00244538
12	2171.35	2175.710276	0.00200979
13	2398.87	2401.307164	0.00101504
14	2412.22	2415.347677	0.00129783
15	3234.06	3239.785086	0.00176982
16	3371.62	3375.162192	0.00105046
17	3885.81	3890.297223	0.00115560
18	4050.25	4056.569782	0.00156152
19	4105.90	4115.19841	0.00226433
20	4356.99	4366.125143	0.00209755
21	4470.20	4485.311388	0.00338144
22	4710.21	4718.908838	0.00184626
23	5083.99	5106.983553	0.00452199
24	5219.66	5264.939322	0.00867563
25	5489.40	5502.236638	0.00233884

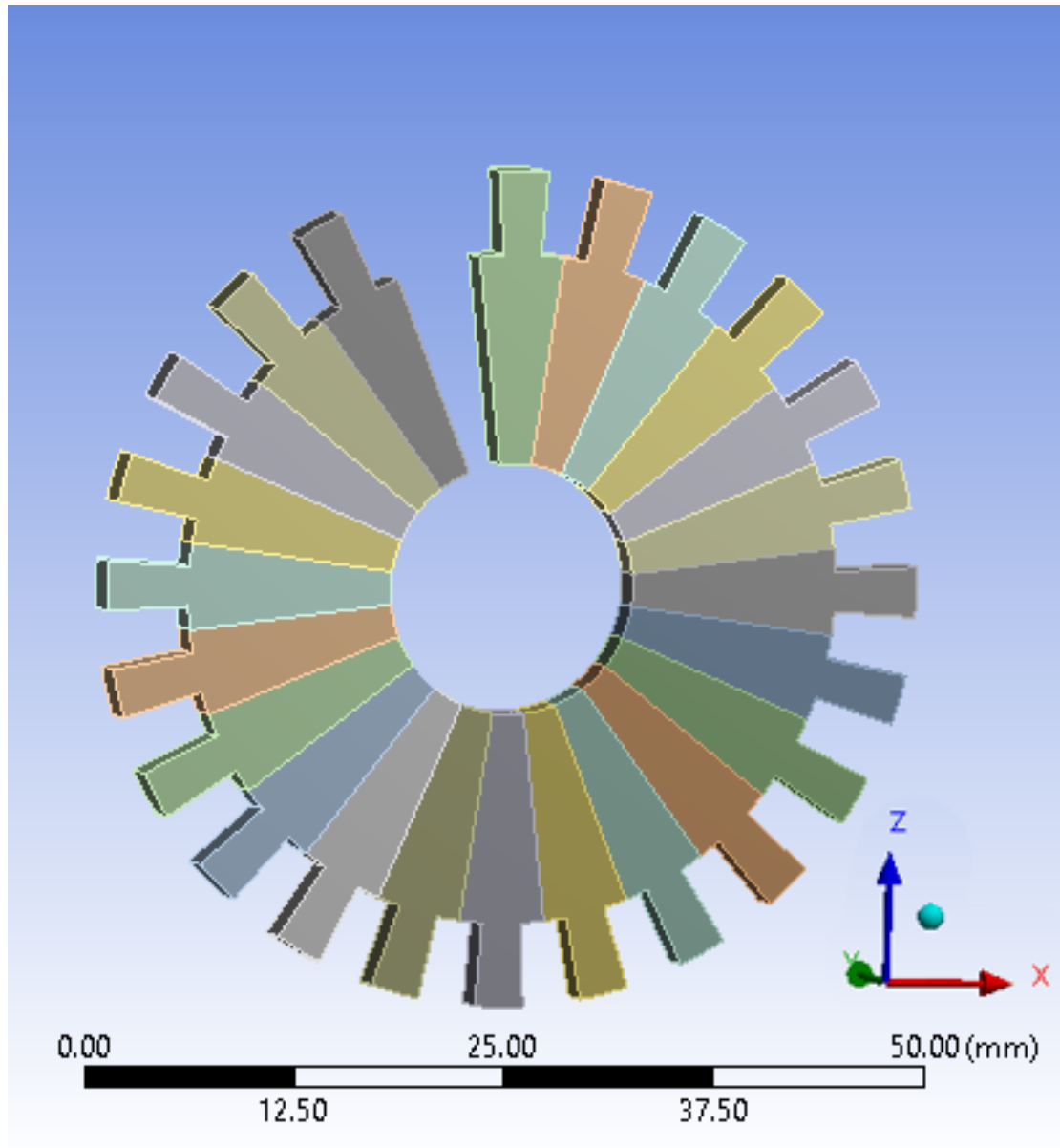


Figure 30: Twenty-three Sectors

	3D Model	1D Model	Error %
1	0.00	0.00	0.00
2	0.00	0.00	0.00
3	0.00	0.00	0.00
4	0.00	0.00	0.00
5	0.00	0.00	0.00
6	0.00	0.00	0.00
7	56.50	56.54152456	0.000783611
8	117.35	117.4469923	0.000835377
9	173.68	173.830403	0.000855743
10	216.46	216.6160197	0.000715841
11	238.32	238.5306039	0.00087575
12	332.61	332.8613465	0.000760601
13	363.50	363.7567992	0.000695955
14	402.27	402.6844372	0.001021932
15	478.14	478.45261	0.000661376
16	517.79	518.1708174	0.000732869
17	595.77	596.1525845	0.000636943
18	663.83	664.2364225	0.000619284
19	745.73	746.2342822	0.000678484
20	764.51	764.9865888	0.00062045
21	800.37	801.194668	0.001027262
22	850.49	851.0637867	0.000669269
23	901.69	902.2926848	0.000666339
24	948.05	948.7149208	0.000700467
25	976.07	976.7643237	0.000712758

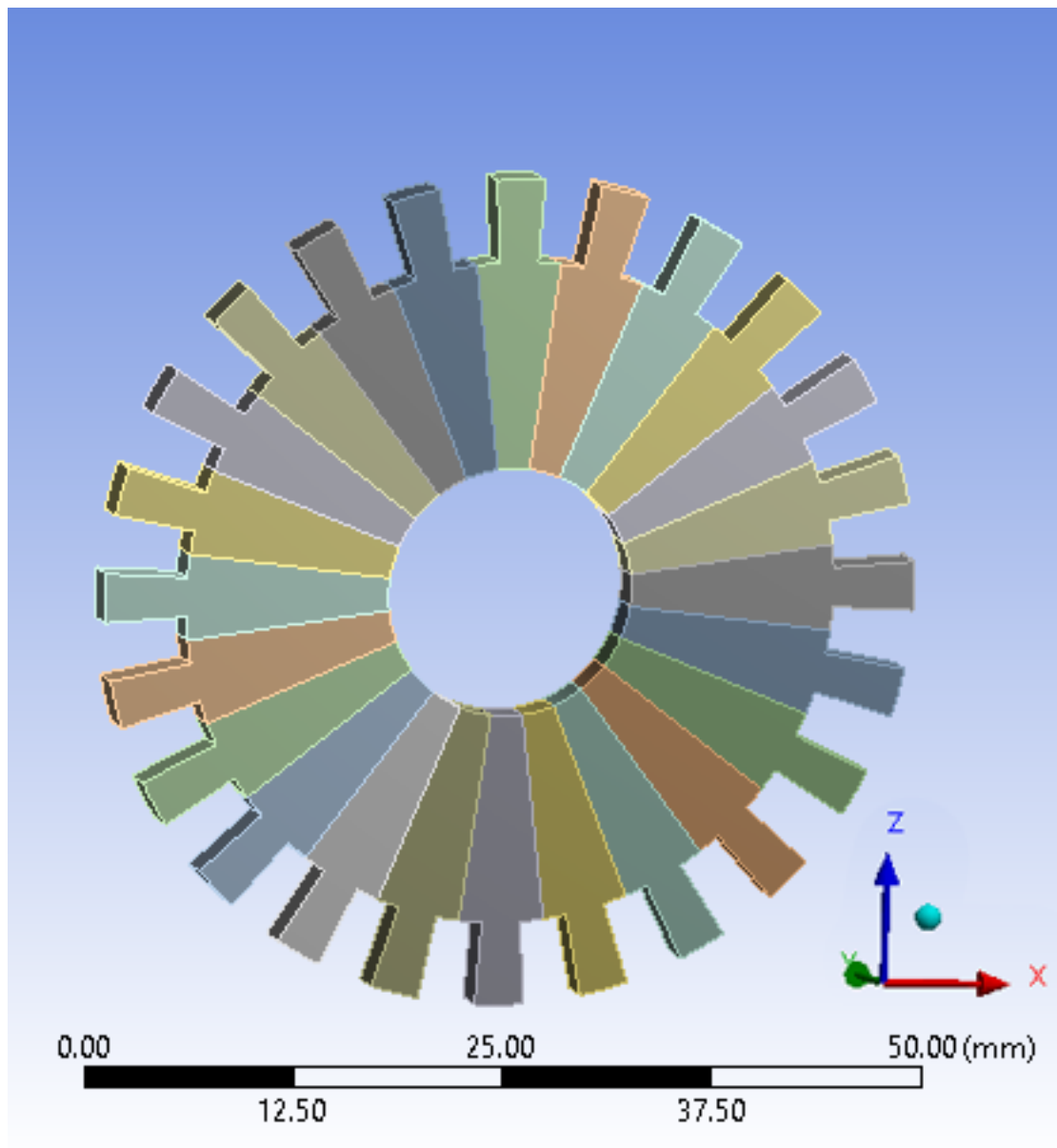


Figure 31: Twenty-four Sectors

Twenty-four sectors were matched. It was important the last one had the nodes of the interface of right matched with the nodes of the interfaces of the left of the first sector. This let to create the full Global Stiffness and Mass Matrices as 3960×3960 matrices. It is possible to examine the shape of these matrices in the following figures:

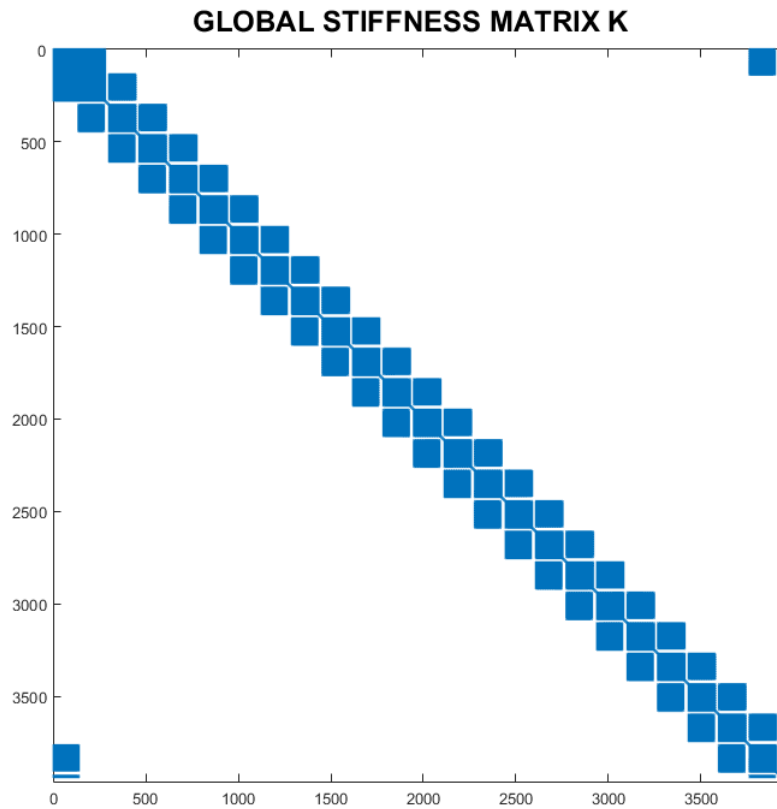


Figure 32: Global Stiffness Matrix K

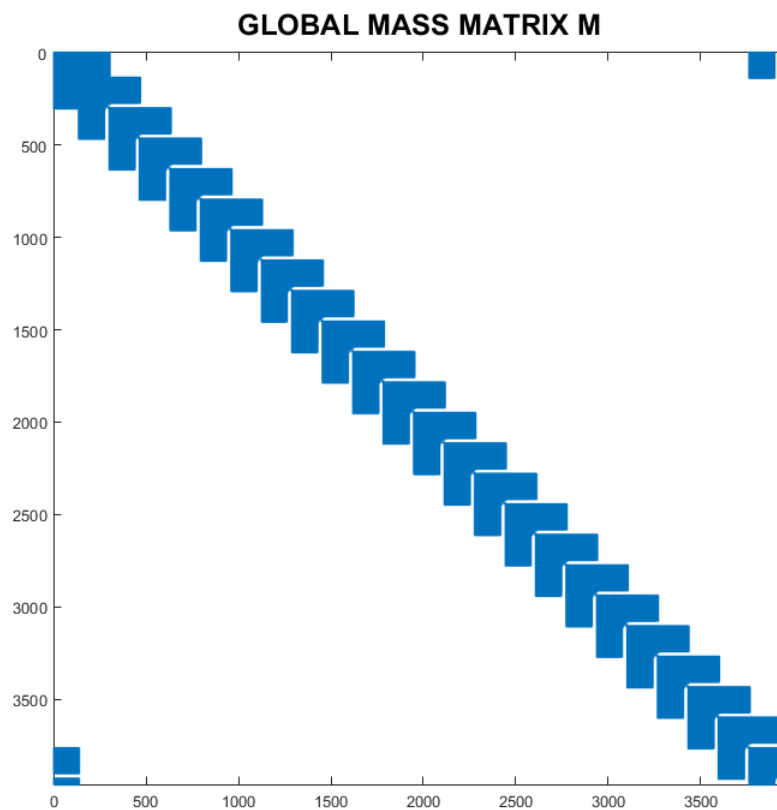


Figure 33: Global Mass Matrix M

	3D Model	1D Model	Error %
1	0.00	0.00	0.00
2	0.00	0.00	0.00
3	0.00	0.00	0.00
4	0.00	0.00	0.00
5	0.00	0.00	0.00
6	0.00	0.00	0.00
7	161.0263407	161.1496696	0.000765892
8	161.0263407	161.1496696	0.000765892
9	283.4317844	283.7195517	0.001015296
10	366.7925858	367.045568	0.000689715
11	366.7925858	367.045568	0.000689715
12	570.2851532	570.601381	0.000554508
13	570.2851532	570.601381	0.000554508
14	570.6330038	571.1073454	0.000831255
15	570.6330038	571.1073454	0.000831255
16	749.5862966	750.0290154	0.000590618
17	749.5862966	750.0290154	0.000590618
18	895.4937878	896.0629978	0.000635638
19	895.4937878	896.0629978	0.000635638
20	919.6852119	920.6338952	0.00103153
21	919.6852119	920.6338952	0.00103153
22	978.5351992	979.2941458	0.000775595
23	978.5351992	979.2941458	0.000775595
24	1007.596531	1008.355477	0.000753225
25	1007.596531	1008.355477	0.000753225

For the complete structure appear again the double frequencies as studied in the first two chapters. Even for the 1D model, this happened and the error between the two models decreased a lot. the difference is about the 0.0007%. This means that it is possible to work on the 1D model without making a big mistake. Let's apply the Mistuning Condition.

The Mistuning condition could be applied for mass or for stiffness. This study lets to analyze what happens if the Mistuning condition is applied in the stiffness matrix K . It will be shown only the case of one sector and full structure. In the detail, it was modified the first element of the stiffness matrix k_{11} .

This element is modified of 5%. This means:

$$k_{11} = 1.05 * k_{11} \quad (3.1)$$

After this modification, the eigenvalues were calculated again to analyze the percentage error. First of all it is showed the differences for the single sector and then for the complete structure.

Table 1: Single Sector

	Frequencies [Hz]	Mistuned Frequencies [Hz]	Error %
1	0.00	0.00	0.000
2	0.00	0.00	0.000
3	0.00	0.00	0.000
4	0.00	0.00	0.000
5	0.00	0.00	0.000
6	0.00	0.00	0.0000
7	1395.165281	1400.00	0.0035
8	1873.21	1879.00	0.0031
9	3195.29	3201.00	0.0018
10	3228.65	3229.00	0.0001
11	3548.96	3555.00	0.0017
12	4724.76	4725.00	0.0001
13	5080.10	5088.00	0.0016
14	5715.85	5722.00	0.0011
15	6370.03	6377.00	0.0011
16	7304.23	7305.00	0.0001
17	8017.16	8022.00	0.0006
18	8526.80	8532.00	0.0006
19	9279.99	9285.00	0.0005
20	10819.29	10820.00	0.0001
21	10899.30	10907.00	0.0007
22	11598.25	11604.00	0.0005
23	12839.04	12839.00	0.0000
24	13394.81	13395.00	0.0000
25	13440.19	13440.00	0.0000

Table 2: Complete Structure

	Frequencies [Hz]	Mistuned Frequencies [Hz]	Error %
1	0.00	0	0
2	0.00	0	0
3	0.00	0	0
4	0.00	0	0
5	0.00	0	0
6	0.00	0	0
7	161.1496696	161.13	0.00093
8	161.1496696	203.38	0.25970
9	283.7195517	296.35	0.04328
10	367.045568	367.03	0.00012
11	367.045568	368.59	0.00260
12	570.601381	571.60	0.00070
13	570.601381	571.62	0.00070
14	571.1073454	571.1	0.00019
15	571.1073454	574.83	0.00506
16	750.0290154	750.04	0.00004
17	750.0290154	750.05	0.00004
18	896.0629978	896.07	0.00007
19	896.0629978	897.2	0.00007
20	920.6338952	921.64	0.00040
21	920.6338952	962.03	0.04493
22	979.2941458	979.30	0.00030
23	979.2941458	979.61	0.00030
24	1008.355477	1008.34	0.00035
25	1008.355477	1008.78	0.00035

As a consequence of Mistuning, the couple for the frequencies has been lost. This is the discrepancy between theory and practice that is occurred in reality when an engine is operating. The fact that the frequencies are not anymore in a couple, means that the structure lost its cyclic symmetry properties in little percentage. The main purpose of a Structural Health Monitoring of the system is to predict these changes during the design of the engine. So, now, the main question is if it is possible to estimate the variation of difference using a difference easier and more immediate method? It will be seen in the next Chapter.

4 Chapter 4

Simplified Calculation of Eigenvalues Derivatives

In chapter 3, the Mistuning condition where applied modifying directly the Mass or Stiffness matrices. Then new eigenvalues of the modified matrices were calculated to find the differences between the non-modified ones. In this chapter is presented an alternative and simpler procedure for the determination of the derivatives of the eigenvalues of n th order algebraic eigensystems. This paper will treat only the case of Derivatives of Eigenvalues. The input elements of this method are one eigenvalue and its right and left eigenvectors. The matrices of the system could be symmetric or non-symmetric. In this procedure, the n th-order ($n-1$) rank system of equations is directly and simply modified to form a system of equations of rank n . This method is exposed by Nelson [11] and Ojalvo [12] respectively for Non-repeated roots and repeated roots condition. First of all, the Nelson procedure will be explained.[13]

4.1 Non-repeated roots

If λ_i is not a repeated root, there are numerous ways for obtaining the eigenvalue gradients. Nelson presents one of the most efficient non-modal expansion methods that preserve the bandwidth of the original system matrices. In the case of the bladed disk of this paper, the case of no-repeated roots coincides with the analysis of the single sector. To start let analyze the eigenvalue equation of finite element analysis of a structure:

$$([K] - \lambda_i[M])\{X_i\} = 0 \quad (4.1)$$

where λ_i represents the natural frequencies and $\{X_i\}$ represents the eigenvectors. The next step is to derive this equation such as:

$$\left(\frac{\delta}{\delta p}\right) ([K] - \lambda_i[M])\{X_i\} = \{0\}$$

This brings to the following equation:

$$([K] - \lambda_i[M]) \left(\frac{\delta X_i}{\delta p}\right) = - \left[\left(\frac{\delta K}{\delta p}\right) - \left(\frac{\delta \lambda_i}{\delta p}\right) M - \lambda_i \left(\frac{\delta M}{\delta p}\right) \right] \{X_i\}$$

From this equation, the derivation of mass matrix is neglectable because the mass matrix is a constant. Furthermore, The eigenvalue derivative is obtained by pre multiplying the equation by $\{X_i\}^T$, as follows:

$$\{X_i\}^T ([K] - \lambda_i[M]) \left(\frac{\delta X_i}{\delta p}\right) = -\{X_i\}^T \left[\left(\frac{\delta K}{\delta p}\right) - \left(\frac{\delta \lambda_i}{\delta p}\right) [M] \right] \{X_i\}$$

This could be done because, in this case, left eigenvectors $\{Y_i\}$ and right eigenvectors $\{X_i\}$ coincide.

Form an overview of this formula is possible to note that the element on the first side of the equation $\{X_i\}^T([K] - \lambda_i[M])$ is zero because represents again the main equation of finite elements. The equation becomes:

$$\{0\} = -\{X_i\}^T \left[\frac{\delta K}{\delta p} \right] \{X_i\} + \{X_i\}^T \left(\frac{\delta \lambda_i}{\delta p} \right) [M] \{X_i\}$$

It is necessary to consider the norm for $\{X_j\}$, usually in the form $\{X_i\}^T [M] \{X_i\} = 1$. This means that the final equation should be:

$$\left(\frac{\delta \lambda_i}{\delta p} \right) = \{X_i\}^T \left[\frac{\delta K}{\delta p} \right] \{X_i\} \quad (4.2)$$

This is the equation to obtain the eigenvalue derivative. To compare the solution with the method in chapter 3 it is needed to derive respect to the same element. It means that the parameter p corresponds to k_{11} . Such as:

$$\left(\frac{\delta \lambda_i}{\delta k_{11}} \right) = \{X_i\}^T \left[\frac{\delta K}{\delta k_{11}} \right] \{X_i\} \quad (4.3)$$

Through a script of Matlab it was possible to compare the two Δ of the difference between the two methods. The two delta are:

$$\Delta \lambda = (\lambda_m - \lambda) \quad (4.4)$$

$$\Delta \lambda_{mistuned} = \left(\frac{\delta \lambda_i}{\delta k_{11}} \right) (0.05 * K_{1,1}) \quad (4.5)$$

The results are displayed below:

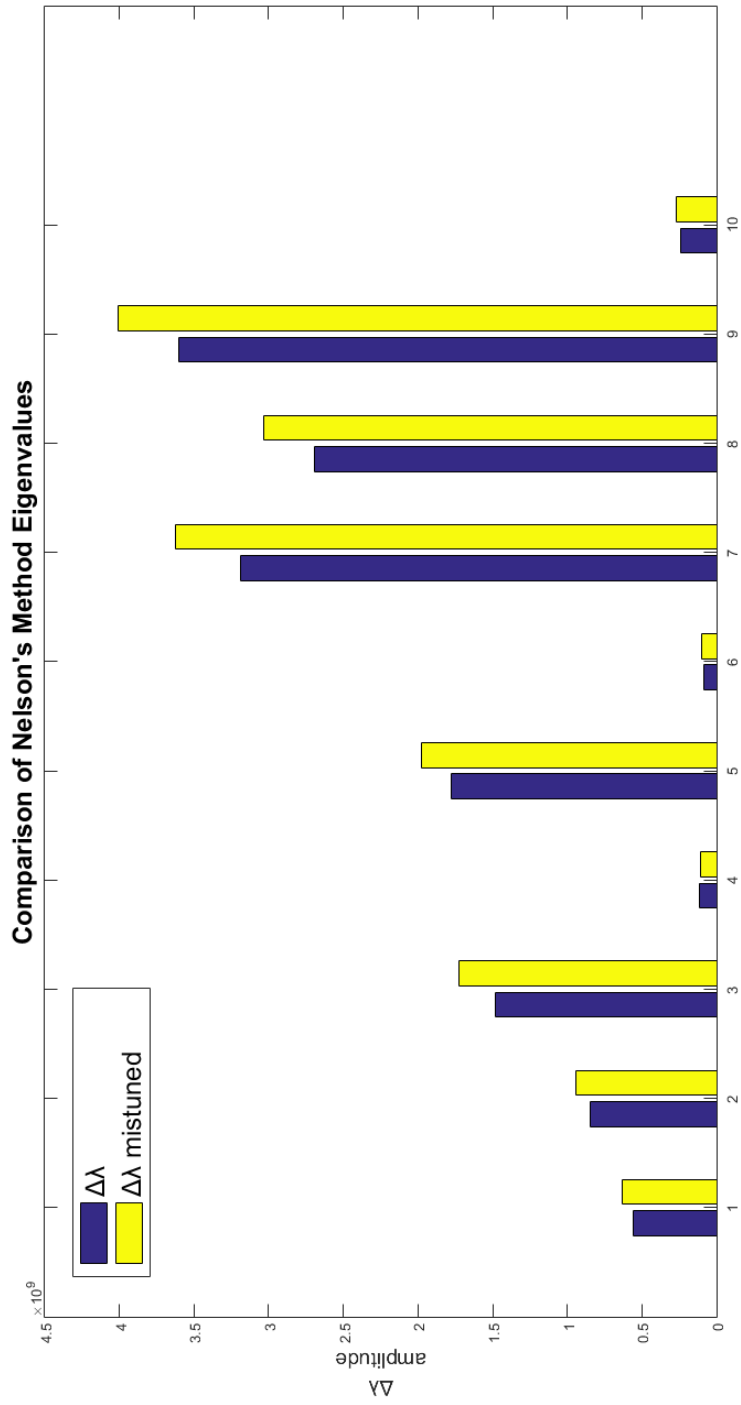


Figure 34: Results of Nelson's Method

4.2 Repeated roots

To develop the Ojalvo's method must follow the same procedure of the Nelson's Method but using the global matrices of Mass and Stiffness. After modified the element K_{11} must care about re-assembling of the Global matrices and applying the same equation:

$$\left(\frac{\delta \lambda_i}{\delta k_{11}} \right)_{full} = \{X_i\}^T \left[\frac{\delta K_{glob}}{\delta k_{11}} \right] \{X_i\} \quad (4.6)$$

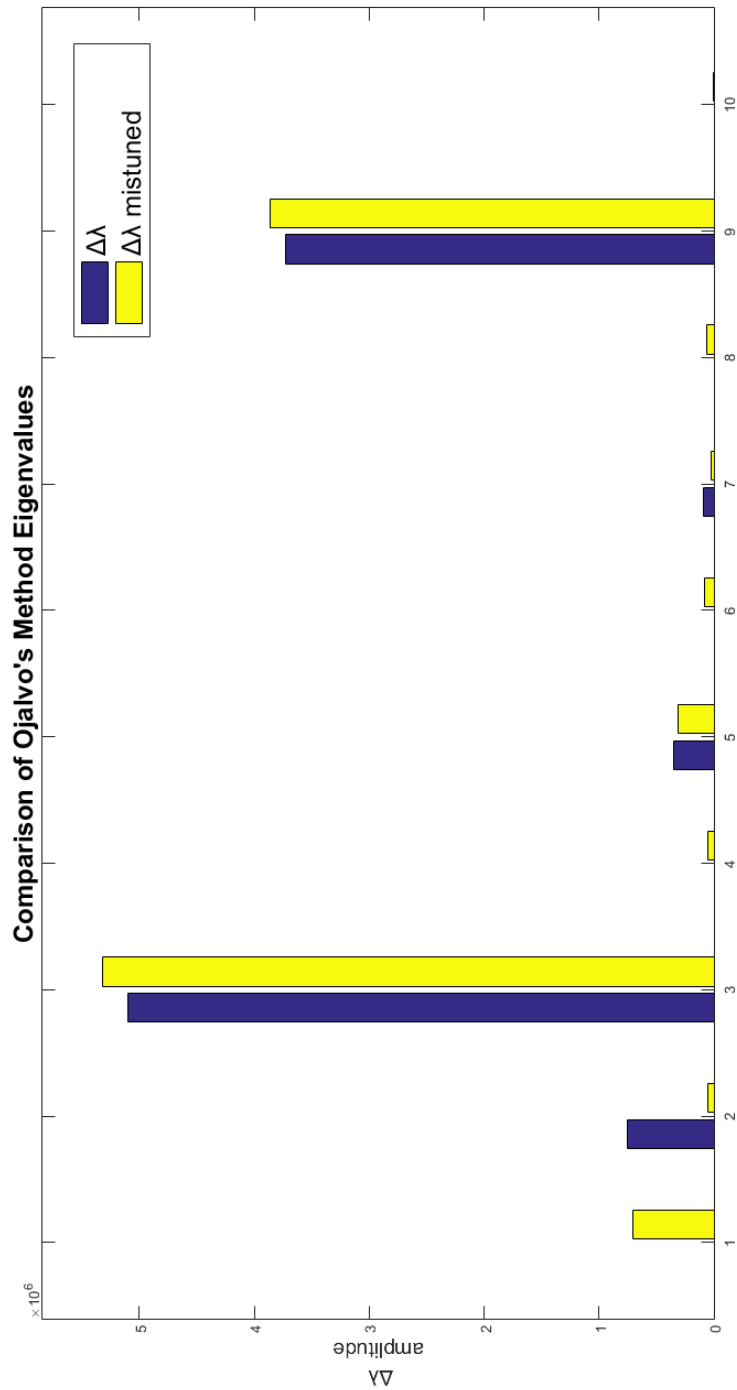


Figure 35: Results of Ojalvo's Method

The analysis of the data of the two graphs show an error between the two delta listed below:

#	Error of Nelson's Method	Error of Ojalvo's Method
1	0	0
2	0	0
3	0	0
4	0	0
5	0	0
6	0	0
7	0.13370107	—
8	0.122298059	0.063628639
9	0.165371843	0.042925821
10	0.049300901	—
11	0.113539144	0.846400336
12	0.154446553	—
13	0.136446583	0.691165108
14	0.123507639	—
15	0.113223659	0.982030555
16	0.124284218	—
17	0.133071572	0.329565806
18	0.119212913	—
19	0.117824633	0.44276883
20	0.243133799	—
21	0.12500031	0.561980694
22	0.114629166	—
23	0.133399562	0.930587701
24	0.168568665	—
25	0.175587786	0.342921357

The Nelson' method shows an average percentage error of about 8% while Ojalvo's one shows an average percentage error of about 4%. It is possible to observe that the error is still little and this demonstrates that to evaluate the mistuned effect on the structure is possible to use the method of eigenvalues derivatives that is faster than the first one and give results acceptable.

5 Conclusion

It is shown in this paper that Modal parameters identified from the measured data represent the dynamic characteristics of a vibrating system and often serve as input to model updating, health monitor or damage diagnosis. To identify the modal parameters of a system, both the excitation force and the response of the system should be measured and the frequency response function between the excitation and the response needs to be calculated. When performing modal analysis one of the key decisions that must be upon starting to analyze the data is to decide how many modes there are in the frequency range of interest.

It was shown how to simulate a Mistuning condition on the bladed disk of a compressor in order to understand how the structure lost his cyclic symmetry. This phenomenon is very dangerous in terms of Safety. For this reason, it is important to predict the mistuning's effects in an easier way. This way was demonstrated in Chapter 4 where two new methods were treated. The results confirmed that the discrepancy between the two philosophy of calculation are similar and this means that is possible to use the fastest methods exposed in Chapter 4, instead of the one exposed in Chapter 3. To better evaluate the effect of the Mistuning it should be important to make analysis also related to the eigenvectors derivatives. But this theme was not treated in this paper.

It was presented that the mistuning jump phenomenon led to significant vibration response localization in the mistuned bladed disk. From a future perspective, this means that must be of primary importance to investigate the trend of Mistuning effects to predict the static and dynamic stresses of the structure in order to avoid the failure of the component.

The tasks reached with this paper could be summed up as:

- To investigate the dynamics of rotationally periodic structure with the FEM benchmark: natural frequencies, mode shapes, and forced responses;
- To verify that a complete structure mistuned model lost his cyclic symmetric properties;
- To show how it is possible to obtain approximately the same results of Mistuning conditions with eigenvalues derivatives methods.

Appendices

A Matlab script

Here is possible to overview the script of matlab that let to obtain the simplified method to calculate eigenvalues derivatives.

Non-repeated roots

```

1 clear all
2 clc
3
4 load('KM.mat');
5 load('Master_Nodes.mat');
6 load('Map.mat');
7
8 % -----
9 [eigVect,lambda] = eig(K,M);
10 [omega_n ip] = sort(diag(sqrt(lambda)));
11 X = eigVect(:,ip);
12 perc=5/100;
13
14 K2=K;
15 K2(1,1)=K2(1,1)*(1+perc);
16 [eigVect2,lambda2] = eig(K2,M);
17 [omega_n2 ip] = sort(diag(sqrt(lambda2)));
18 X2 = eigVect2(:,ip);
19
20
21 dK = zeros(300);
22 dK(1,1)=1; %variazione rispetto al primo valore diagonale k11
23 n=25;
24 i=1;
25 for i=1:n
26     DELTA1(i)=lambda2(i,i)-lambda(i,i);
27     dlambd(i)=X(1,i)^2;
28     DELTA2(i)=dlambd(i)*(K(1,1)*perc);
29     fprintf(1,'%12.0f %12.0f %12.0f %12.0f\n',lambda(i,i),lambda2(i,i),DELTA1(i),DELTA2(i));
30     i=i+1;
31 end

```

Repeated roots

```

1 clear all
2
3 load('KM.mat');
4 load('Master_Nodes.mat');
5 load('Map.mat');
6
7 % -----
8 % [eigVect,lambda] = eig(M\K);
9 [eigVect,lambda] = eig(K,M);
10
11 [omega_n ip] = sort(diag(sqrt(lambda/1000)));
12
13 Psi = eigVect(:,ip);

```

```

14 % -----
15 % sector dof
16 Ndof_sect = length(K);
17
18 % interface dof
19 Ndof_int = length(dof_intL);
20
21 % Number of sectors
22 nsec = 24;
23
24 % Number of modes
25 Nmodes = 24;
26
27 % -----
28 % -----
29 %
30 % Global stiffness matrix tuned disk
31 N = nsec*(Ndof_sect - Ndof_int);
32 K_glob = zeros(N,N);
33 M_glob = zeros(N,N);
34
35 % -----
36 % -----
37 % First sector unchanged
38 K_glob(1:Ndof_sect,1:Ndof_sect) = K;
39 M_glob(1:Ndof_sect,1:Ndof_sect) = M;
40
41 % -----
42 % Sectors from second to the second-last
43 for ns = 2:nsec-1
44
45     map_mtrx(1:Ndof_int) = dof_intR + (ns-2)*(Ndof_sect - Ndof_int);
46     map_mtrx(Ndof_int+1:2*Ndof_int) = T_dofs + (ns-1)*(Ndof_sect - Ndof_int);
47     map_mtrx(2*Ndof_int+1:2*Ndof_int+3) = ID_F + (ns-1)*(Ndof_sect - Ndof_int);
48     map_mtrx(2*Ndof_int+4:2*Ndof_int+6) = ID_R + (ns-1)*(Ndof_sect - Ndof_int);
49     map_mtrx(2*Ndof_int+7:Ndof_sect) = [2*Ndof_int+7:1:Ndof_sect]+ (ns-1)*(Ndof_sect - Ndof_int);
50
51     for i = 1:length(map_mtrx)
52         irow = map_mtrx(i);
53
54         for j = 1:length(map_mtrx)
55             jcol = map_mtrx(j);
56             K_glob(irow, jcol) = K_glob(irow, jcol) + K(i, j);
57             M_glob(irow, jcol) = M_glob(irow, jcol) + M(i, j);
58         end
59     end
60 end
61
62 end
63
64 % -----
65 % Assembling the last sector
66 ns = nsec;
67
68 map_mtrx(1:Ndof_int) = dof_intR + (ns-2)*(Ndof_sect - Ndof_int);
69 map_mtrx(Ndof_int+1:2*Ndof_int) = dof_intL;
70 map_mtrx(2*Ndof_int+1:2*Ndof_int+3) = ID_F - Ndof_int + (ns-1)*(Ndof_sect - Ndof_int);
71 map_mtrx(2*Ndof_int+4:2*Ndof_int+6) = ID_R - Ndof_int + (ns-1)*(Ndof_sect - Ndof_int);
72 map_mtrx(2*Ndof_int+7:Ndof_sect) = [2*Ndof_int+7:1:Ndof_sect] - Ndof_int + (ns-1)*(Ndof_sect - Ndof_int);
73
74 for i = 1:length(map_mtrx)
75     irow = map_mtrx(i);
76
77     for j = 1:length(map_mtrx)
78         jcol = map_mtrx(j);
79         K_glob(irow, jcol) = K_glob(irow, jcol) + K(i, j);

```

```

80         M_glob(irow, jcol) = M_glob(irow, jcol) + M(i, j);
81     end
82
83     end
84 % -----
85 % -----
86
87 [eigVect, lambda] = eig(K_glob, M_glob);
88
89 % % % lambda = diag(lambda);
90 % % %
91 % % % [omega_n ip] = sort(diag(sqrt(lambda)));
92
93 lambda = diag(lambda);
94 [omega_n ip] = sort(sqrt(lambda/1000));
95 lambda = lambda(ip);
96
97 Psi = eigVect(:, ip);
98 f = omega_n/2/pi;
99
100 fprintf(1, '%10.0f\n', real(f(1:25)));
101 % -----
102 % -----
103 % -----
104 %
105 % Global stiffness matrix mituned disk
106 N = nsec*(Ndof_sect - Ndof_int);
107 K_globMT = zeros(N,N);
108 M_globMT = zeros(N,N);
109
110 % -----
111 % -----
112 % First sector unchanged
113 K_globMT(1:Ndof_sect, 1:Ndof_sect) = K;
114 M_globMT(1:Ndof_sect, 1:Ndof_sect) = M;
115
116 perc= 5/100;
117 K_globMT(1,1)=K_globMT(1,1)*(1+perc);
118
119 % -----
120 % Sectors from second to the second-last
121 for ns = 2:nsec-1
122
123     map_mtrx(1:Ndof_int) = dof_intR + (ns-2)*(Ndof_sect - Ndof_int);
124     map_mtrx(Ndof_int+1:2*Ndof_int) = T_dofs + (ns-1)*(Ndof_sect - Ndof_int);
125     map_mtrx(2*Ndof_int+1:2*Ndof_int+3) = ID_F + (ns-1)*(Ndof_sect - Ndof_int);
126     map_mtrx(2*Ndof_int+4:2*Ndof_int+6) = ID_R + (ns-1)*(Ndof_sect - Ndof_int);
127     map_mtrx(2*Ndof_int+7:Ndof_sect) = [2*Ndof_int+7:1:Ndof_sect]+ (ns-1)*(Ndof_sect - Ndof_int);
128
129     for i = 1:length(map_mtrx)
130         irow = map_mtrx(i);
131
132         for j = 1:length(map_mtrx)
133             jcol = map_mtrx(j);
134             K_globMT(irow, jcol) = K_globMT(irow, jcol) + K(i, j);
135             M_globMT(irow, jcol) = M_globMT(irow, jcol) + M(i, j);
136         end
137     end
138 end
139
140 end
141
142 % -----
143 % Assembling the last sector
144 ns = nsec;
145

```

```

146 map_mtrx(1:Ndof_int) = dof_intR + (ns-2)*(Ndof_sect - Ndof_int);
147 map_mtrx(Ndof_int+1:2*Ndof_int) = dof_intL;
148 map_mtrx(2*Ndof_int+1:2*Ndof_int+3) = ID_F - Ndof_int + (ns-1)*(Ndof_sect - Ndof_int);
149 map_mtrx(2*Ndof_int+4:2*Ndof_int+6) = ID_R - Ndof_int + (ns-1)*(Ndof_sect - Ndof_int);
150 map_mtrx(2*Ndof_int+7:Ndof_sect) = [2*Ndof_int+7:1:Ndof_sect] - Ndof_int + (ns-1)*(Ndof_sect - Ndof_int);
151
152 for i = 1:length(map_mtrx)
153     irow = map_mtrx(i);
154
155     for j = 1:length(map_mtrx)
156         jcol = map_mtrx(j);
157         K_globMT(irow,jcol) = K_globMT(irow,jcol) + K(i,j);
158         M_globMT(irow,jcol) = M_globMT(irow,jcol) + M(i,j);
159     end
160
161 end
162 % -----
163 % -----
164
165 [eigVectMT,lambdaMT] = eig(K_globMT,M_globMT);
166
167 lambdaMT = diag(lambdaMT);
168 [omega_nMT ip] = sort(sqrt(lambdaMT/1000));
169 lambdaMT = lambdaMT(ip);
170
171 PsiMT = eigVectMT(:,ip);
172 fMT = omega_nMT/2/pi;
173
174 fprintf(1, '%10.0f\n', real(fMT(1:25)));
175 % -----
176
177 lambdaMT = real(lambdaMT);
178 lambda = real(lambda);
179
180 for i = 7:25
181     Deltalambda(i) = lambdaMT(i)-lambda(i);
182     der_lambda(i) = real(Psi(1,i)^2);
183     DK11 = K(1,1)*perc;
184     Dlambd(i) = real(der_lambda(i)*DK11);
185     fprintf(1, '%12.0f %12.0f %12.0f %10.0f\n', lambda(i), lambdaMT(i), Deltalambda(i), Dlambd(i));
186 end
187
188 ip = [1 2 3 4 5 6 8 7 9 11 10 12 13 15 14 16 17 18 19 20 21 22 23 24 25];
189
190 y=[abs(Deltalambda'), Dlambd(ip)'];
191
192 bar(y(7:16,:));

```


References

- [1] D.L.Thomas, 'Dynamic of Rotationally Periodic Structures' *International Journal For Numerical Methods In Engineering*, VOL. 14,81-102 (1979)
- [2] *Lumped and Consistent Mass Matrices*
- [3] J.Yuan, G.Allegri, F. Scarpa, R. Rajasekaran, S. Patsias, 'Probabilistic dynamics of mistuned bladed disc systems using subset simulation' *Journal of Sound and Vibration* , 5 May 2015
- [4] G.S. Ottarsson, 'DYNAMIC MODELING AND VIBRATION ANALYSIS OF MISTUNED BLADED DISKS' , University of Michigan, 3 Jun 2011
- [5] Dr. Sondipon Adhikari, 'Vibration of Damped Systems' *Master's Thesis* , University of Bristol
- [6] J.D.Marcias, J.J.Alvarado-Gil, J.Ordonez-Miranda, 'Resonance frequencies and Young's modulus determination of magnetorheological elastomers using the photoacoustic technique' *Journal of Applied Physics*, December 2012
- [7] C.Breard, J.S.Green, M.Imregun, 'Low-Engine-Order Excitation Mechanisms in Axial-Flow Turbomachinery' *Journal of Propulsion And Power*,Vol.19, No 4, July-August 2003
- [8] H.Liao, J.Wang, J.Yao, Q.Li, 'Mistuning Forced Response Characteristics Analysis of Mistuned Bladed Disks' *Journal of Engineering for Gas Turbines and Power*, DECEMBER 2010, Vol. 132
- [9] M.P.Castanier, C.Pierre 'Modeling and Analysis of Mistuned Bladed Disk Vibration: Status and Emerging Directions' *Journal of Engineering for Gas Turbines and Power*, Vol. 22, No. 2, March–April 2006
- [10] S.Willeke, L.P. Scheidt, J.Wallaschek 'Reduced Order Modeling of Mistuned Bladed Disks under Rotation' *TECHNISCHE MECHANIK*,April 12, 2017
- [11] Richard B. Nelson, 'Simplified Calculation of Eigenvector Derivatives' *AIAA JOURNAL*, VOL. 14,NO.9, September 1976
- [12] I.U.Ojalvo, 'Efficient Computation of Modal Sensitivities for Systems with Repeated Frequencies' *AIAA JOURNAL*, VOL. 26,NO.3, March 1988
- [13] Nico van der Aa, 'Computation of eigenvalue and eigenvector derivatives for a general complex-valued eigensystem' , October, 2006